Limmat Scientific

Instrumentation for Turbomachinery Application

問い合わせ先：(株)インターナショナル・サーボ・データー
Tel：03-6382-4350　e-mail：measure@isdsystems.co.jp

A Spin off company of:

ETH
Eidgenössische Technische Hochschule Zürich
Swiss Federal Institute of Technology Zurich

Limmat Scientific AG, Industriestrasse 7, CH-6300 Zug, Switzerland

Limmat Scientific社

- ETH（チューリッヒ工科大学）の分離独立会社
- 流体用センサー、計測技術、流体力学コンピュータ解析、技術供与

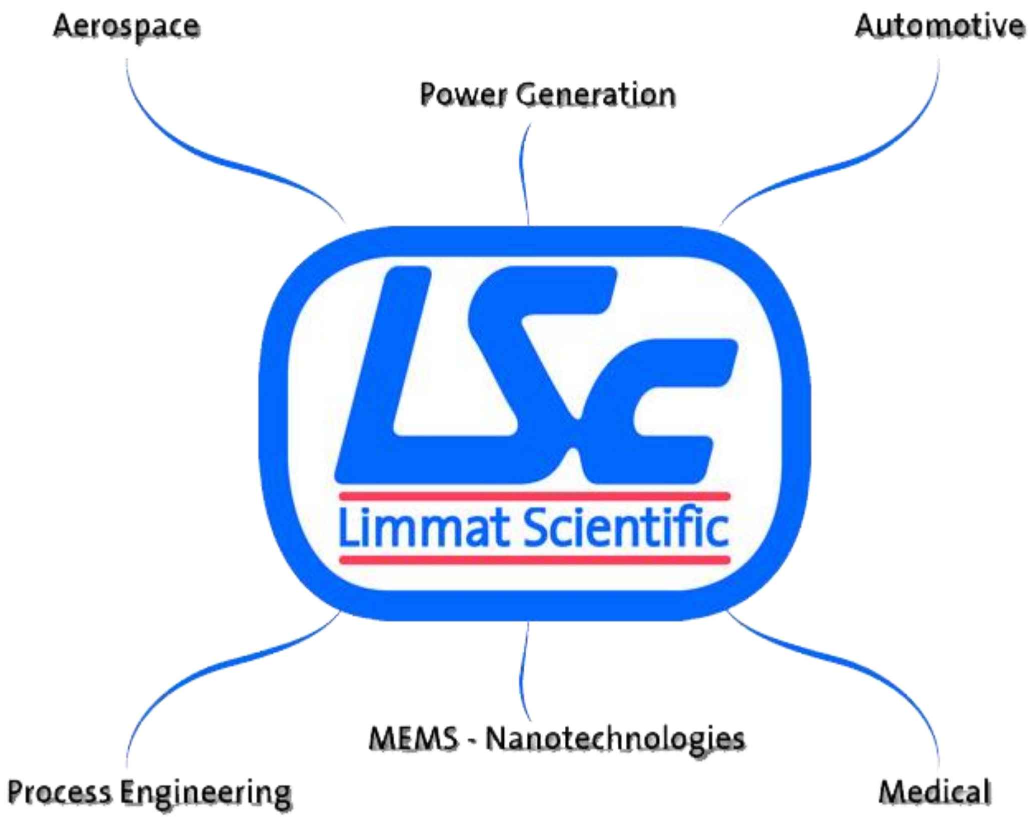

概要

- 標準流体用プローブ
  - 空力用プローブ (5孔/4孔)
  - 高応答流体用プローブ(FRAP)
  - ターンキーシステム 及び データ処理ソフトウエアー
- 多チャンネルセンサー用 テレメトリーシステム
  - 高応答センサー（air, water & steam用）
  - エレクトロニクス（データロガー、その他）内蔵
- 粒子含有流体用計装
  - FRAP-HTH for wet steam flowfield measurement
  - FRAP-OB for coarse particles measurement
  - FRAP-OE for fog droplets measurement
- キャリブレーション施設 及び サービス

Standard Probe Technology
標準プローブ技術

Pneumatic 5HP Probe Technology

- Steady 5 hole probe
  - **Minimal tip diameter: 0.9mm for minimal blockage and maximum spatial resolution**
  - Cobra, L-shaped or stem
  - Robust design: up to 550° C and routinely used up to Mach = 0.9)
  - High accuracy

- Measurement Capabilities
  - **P_o, P_s, φ (yaw), γ (pitch), Mach**
  - **P_o:±80Pa, P_s:±90Pa**
  - Dense measurement grid: typically 45 x 60 points
  - Power performance measurement

Pneumatic 4HP Probe Technology

- Steady 4-hole probe
  - **Minimum tip diameter: 1.8**
  - Stem probe
  - Robust design (up to 600° C)
  - High accuracy

- Measurement Capabilities
  - **P_o, P_s, φ (yaw), γ(pitch), Mach**
  - **P_t:±80Pa, P_s:±90Pa**
  - Power performance measurement

  - **Also provide: boundary layer probes, 3-hole probes and total temperature probes**

Fast-Response Aerodynamic Probe – Standard Temperature

- **Model: FRAP-ST-2S**
  - Miniature Size: **1.8mm in diameter**
  - **2 encapsulated piezo-resistive Die**
  - Virtual 4-sensor mode
  - Routinely used in power generation & aircraft engine industrial test facilities

- Measurement Capabilities
  - **Unsteady P_t, P_s, φ, γ, M, V isotropic turbulence, vorticity**
  - $T_{max} = 120^\circ$ C
  - **Measurement Bandwidth: 48kHz (uncompensated)**

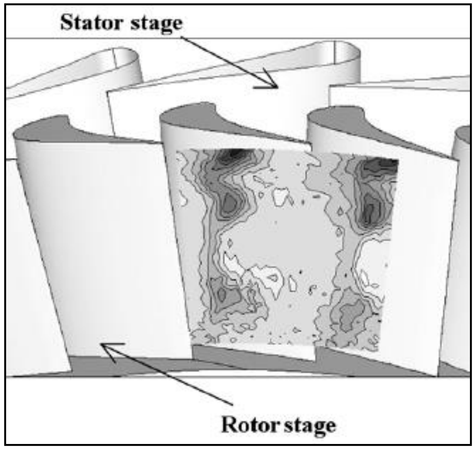

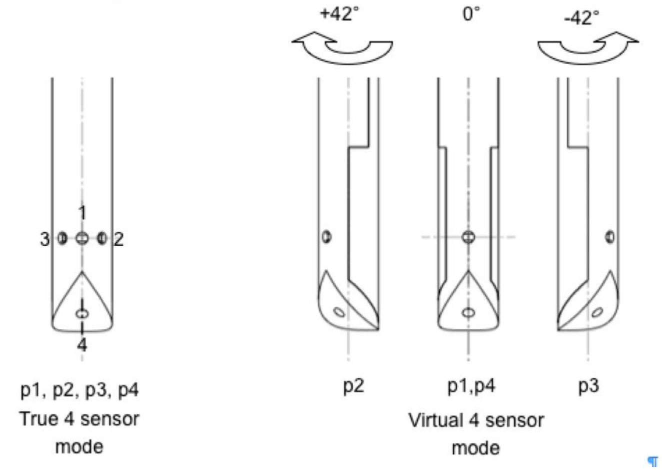

Fast-Response Aerodynamic Probe – High Temperature

- **Model: FRAP-ST-2S**
  - Probe tip Ø 2.5mm
  - **Temperature Range up to 220° C**
  - Unsteady Pressure and Velocity Field
  - Measurement bandwidth 25 kHz (uncompensated)
  - Steady Temperature (1 Hz)
  - **Unsteady P_T, P_s, yaw and pitch flow angles, Mach, turbulence, vorticity**

- Applications
  - High speed Radial compressor @ design and off-design points Mu = 1.33
  - Hot streak measurement campaigns with engine representative dimensional parameters
  - Unsteady inlet flow distortion in aggressive S-duct design on axial compressor performance (aircraft engine development program)

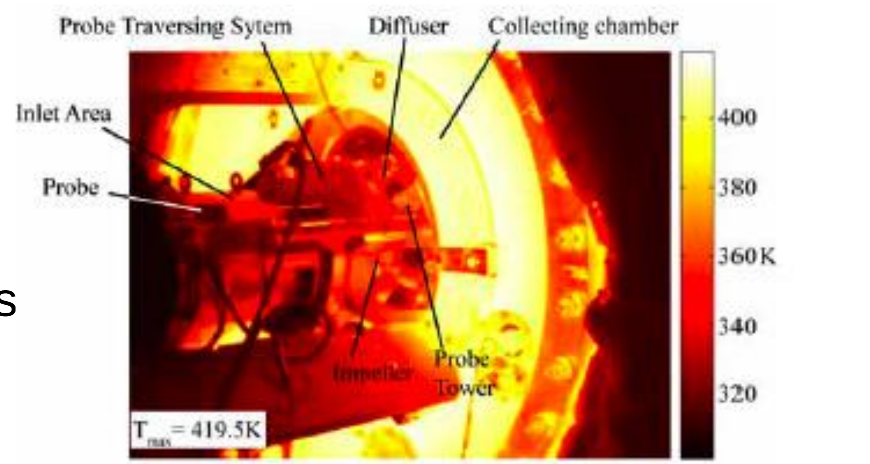

.8-5 *Exemplary temperature distribution of the RIGI facility outer casing surface during operation at Mu=1.33, taken by an IR camera.*

New Development: FRAP-ST-4S / FRAP-HT-4S

- Probe tip Ø 4/5mm **equipped with 4 sensors**
- **Temperature Range:**
  - **ST- type: 120 ° C**
  - **HT- type: 220° C**
- Unsteady Pressure and Velocity Field
- Measurement bandwidth:
  - ST type: 48 kHz
  - HT type: 25 kHz
- Steady Temperature (1 Hz)
- **Unsteady P_T, P_s, T_T, φ, γ, M, V**
- **Non-Isotropic turbulence measurement, shear stress components**

- **Applications: Fan aerodynamics (real size turbofan engine)**

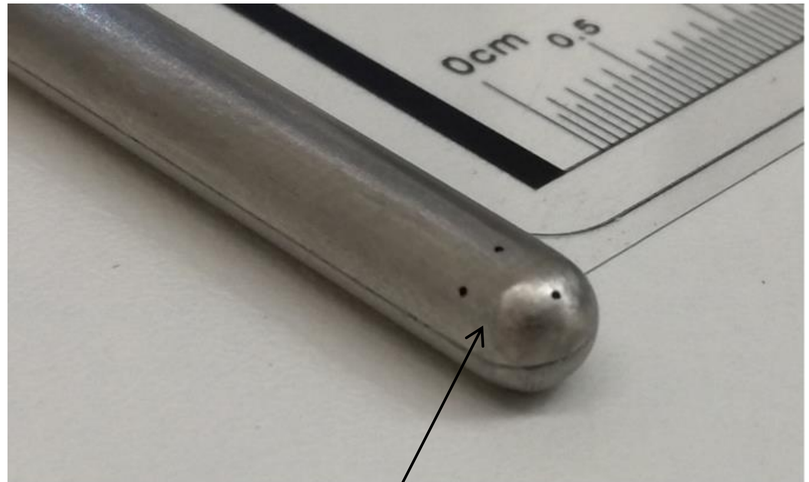

4-sensors installed in tip of Ø 5mm

Turn-Key Measurement System

- **Novel pneumatic & fast-response Probes**
- **Integrated calibration**
- **Data acquisition and control tower**
- **Traversing system, 2 or 3-axis**
- **Software for :**
    - **Data acquisition and monitoring**
    - **Data reduction**
    - **Data visualization**

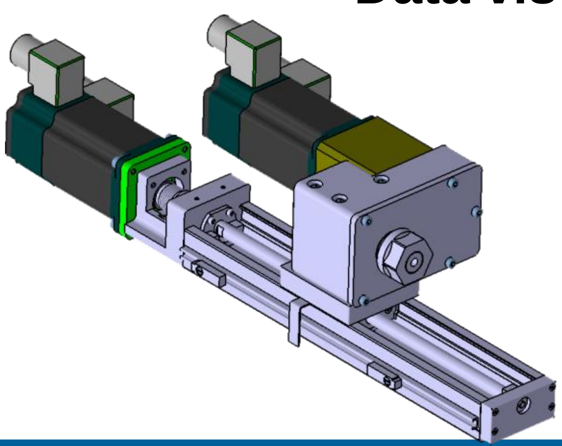

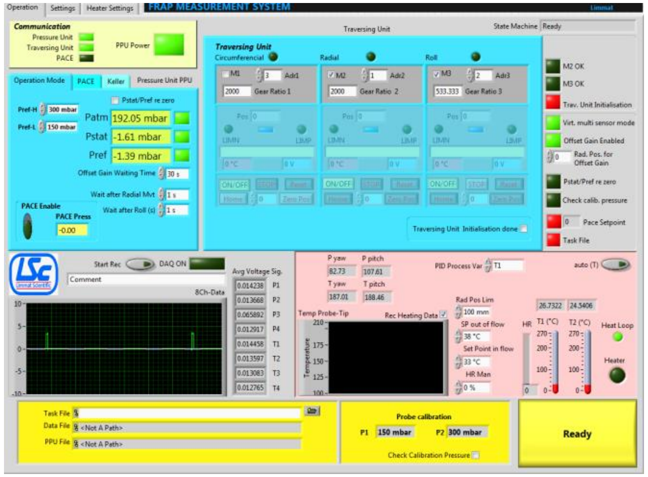

Data ACQ & Monitoring GUI (4HP & 5HP)

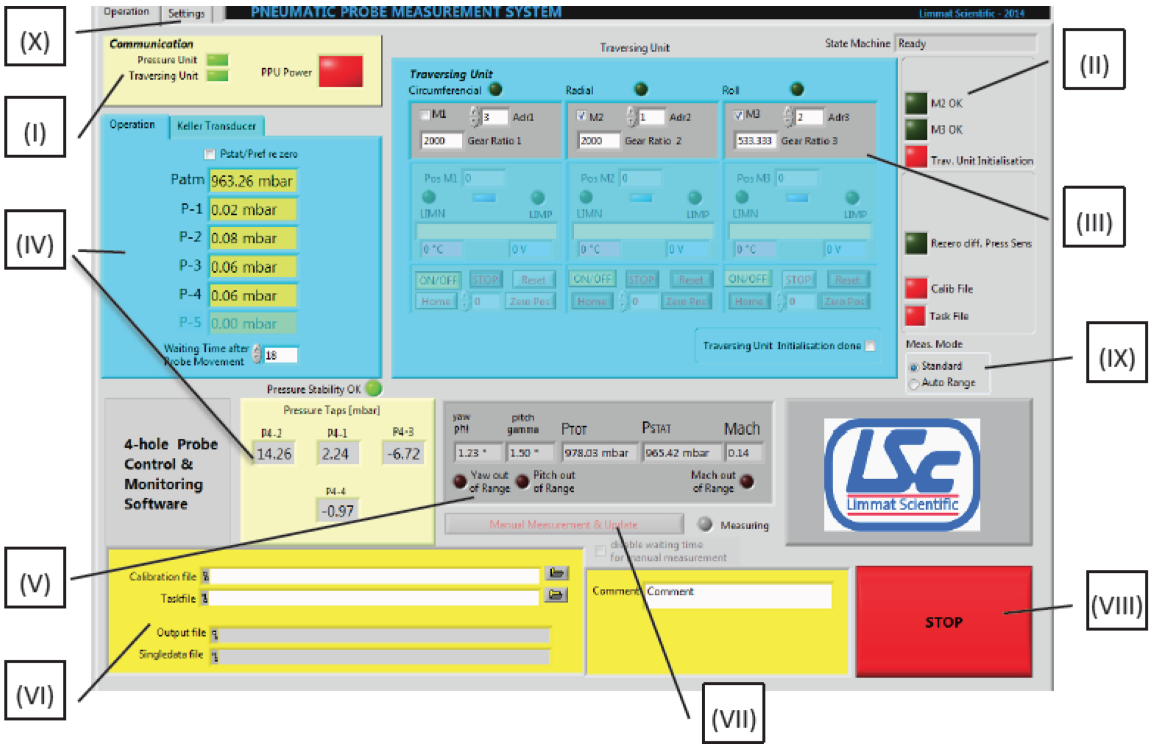

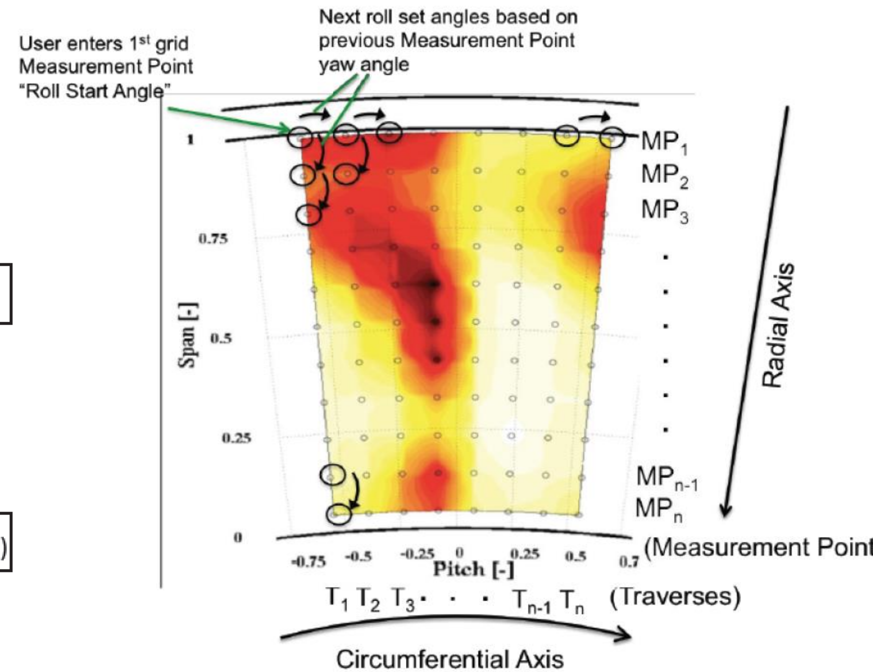

- User friendly interface (system initialization, file management, system status)
- 3-axis automated traversed (radial, yaw, circumfercencial)
- Fully Automated yaw search in unknow flowfield
- Realtime flow condition monitoring

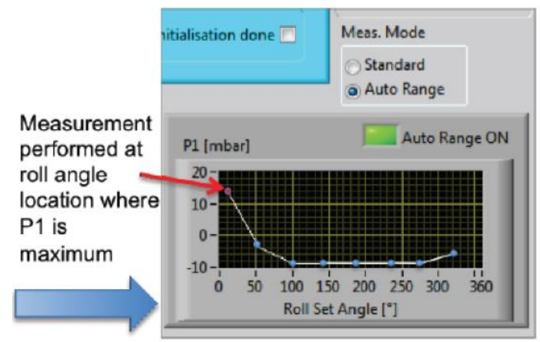

Data ACQ & Monitoring GUI (FRAP)

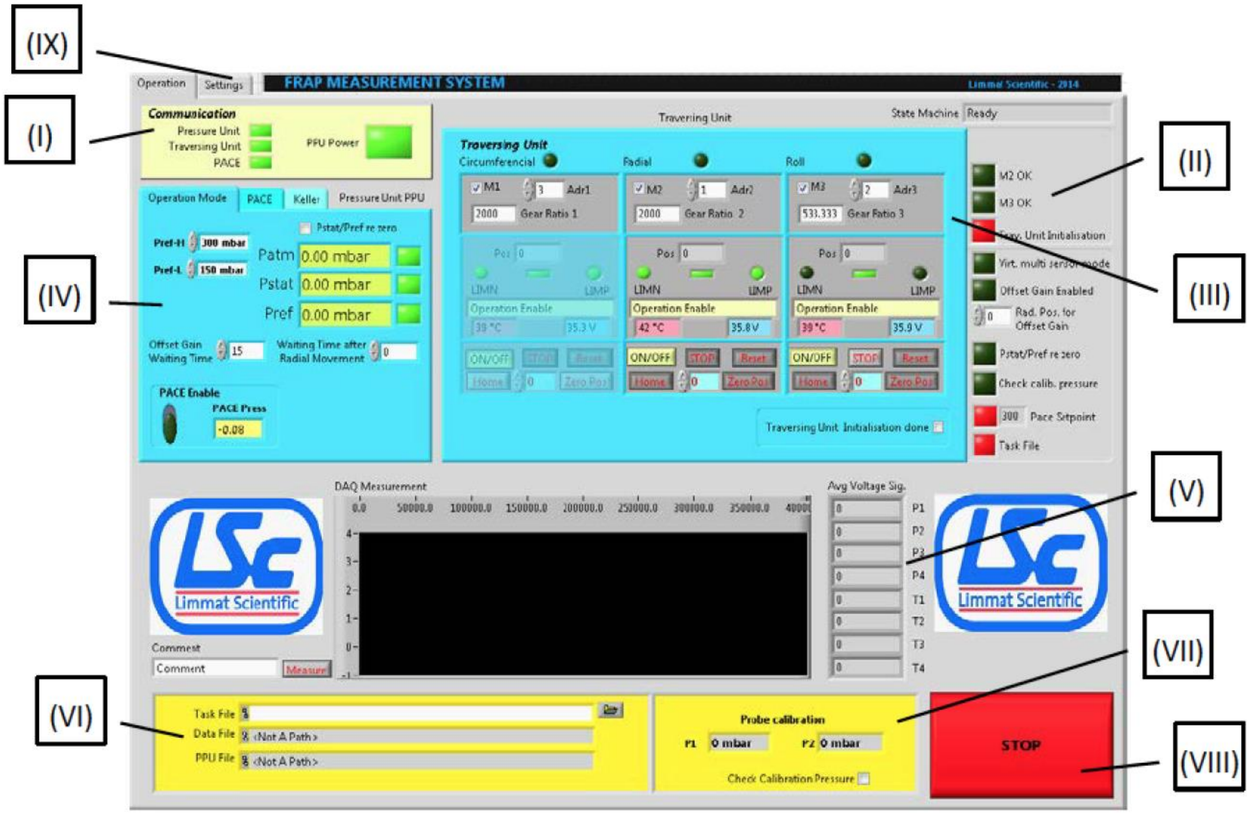

- User friendly interface (system initialization, file management, system status)
- 3-axis automated traverse (radial, yaw, circumferential)
- Realtime fast signal monitoring

Data Reduction Software

100GB binary raw data

User input

FRAP raw data (time-resolved)

Rig monitoring data (time-averaged)

STEP 1: Phase Lock Data
Read FRAP raw data
Phase-lock data with rotor trigger
Pressure sensor signal conversion

STEP 2: Time-resolved Flow Quantities
Pressure into Flow quantities
Phase-lock averaging of flow quantities
Turbulent flow quantities

STEP 3: Postprocessor
Time-average flow quantities (1D)
Time-distance (2D)
Flow quantities animation movie (3D)

3hours data reduction

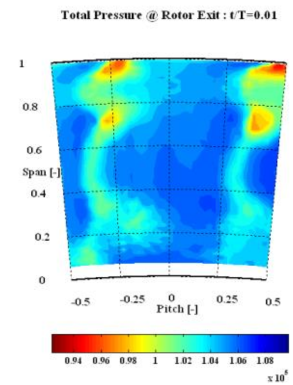

Computationally time-efficient data reduction code with minimum user interaction

Post-Processing Tool

- Single Point or Traverse Analysis, including FFT (1D)
- Distance - Diagrams in both directions, Radial & Circumference (2D)
- Field Traverse Analysis inclusive Secondary Flow Velocity Field (3D)
- Diverse Animation Movies of the unsteady Flow Field

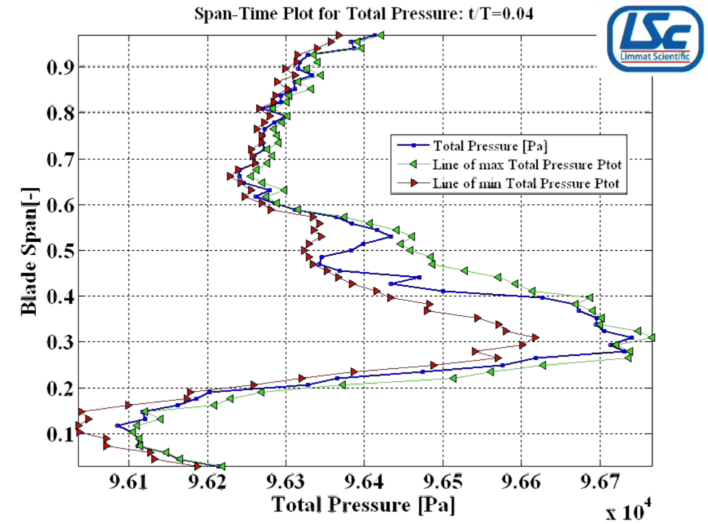

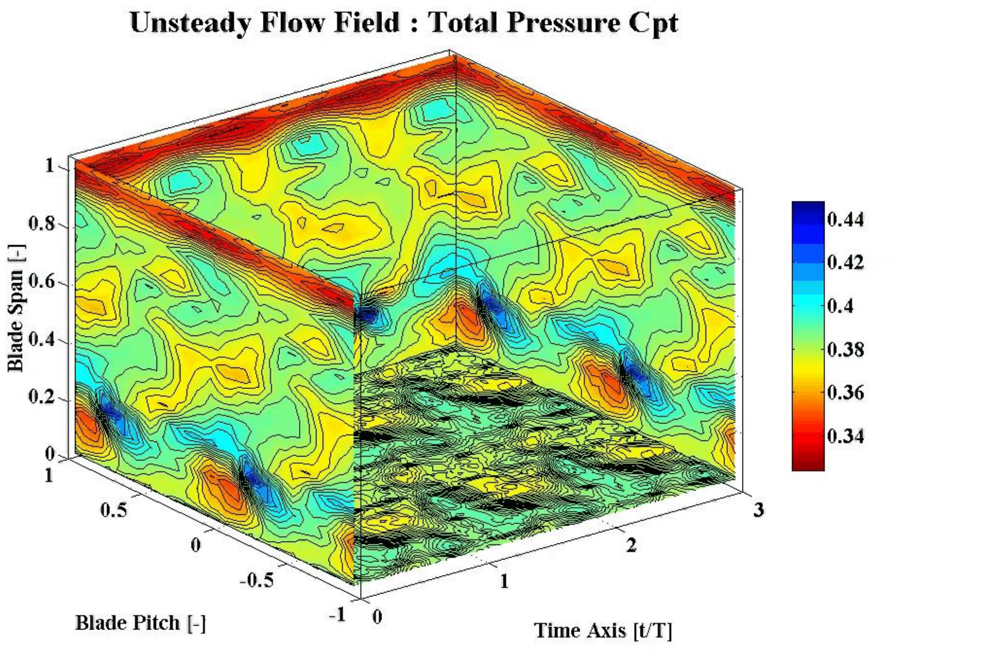

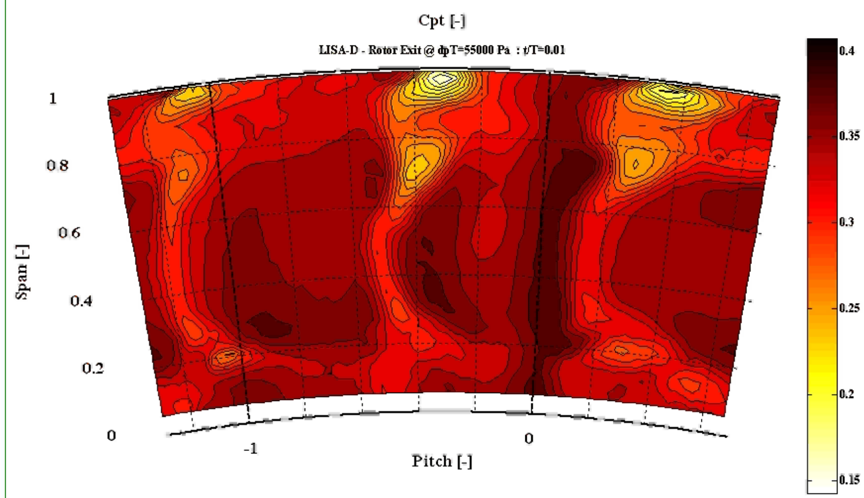

Post-Processing Tool

Available flow quantities

```
'Flow angle Phi local [°]', ...
'Flow angle Gamma local [°]', ...
'Total pressure Ptot [Pa]', ...
'Static pressure Pstat [Pa]', ...
'Isentropic Mach number [-]', ...
'Total temperature [°C] (recovery)', ...
'Total pressure coefficient Cpt [-]', ...
'Static pressure coefficient Cps [-]', ...
'Flow angle Phi global [°]', ...
'Flow angle Gamma global [°]', ...
'Velocity vector plot Vx [m/s]', ...
'Velocity vector plot Vr [m/s]', ...
'Velocity vector plot Vtheta [m/s]', ...
'Relative Mach number [-]', ...
'Flow angle Phi relative [°]', ...
'Relative total pressure coefficient Cpt [-]', ...
'Velocity vector plot Vtheta relative [m/s]', ...
```

```
'Level of stochastic unsteadiness P1prime RMS [mbar]', ...
'P1 pressure [mbar]', ...
'P2 pressure [mbar]', ...
'P3 pressure [mbar]', ...
'u''/c [%]', ...
'v''/c [%]', ...
'w''/c [%]', ...
'Shear stress u''v''/c^2 [-]', ...
'Shear stress u''w''/c^2 [-]', ...
'Shear stress v''w''/c^2 [-]', ...
'Tu c iso [%]', ...
'Tu u''+w'' [%]', ...
'Tu u''+w''+v'' [%]'};
```

Time-resolved Measurements in LEC-ETHZ Axial Turbine

- Measurements conducted in 1-1/2 stage unshrouded axial turbine LISA of the Laboratory for Energy Conversion at ETH Zurich
- Open test case data configuration measured with 2-sensor FRAP probe (describe on slide 9)
- Axial turbine characteristics

Rotor speed [RPM]	2700
Pressure ratio (1.5-Stage, total-to-static)	1.60
Turbine entry temperature [°C]	55
Total inlet pressure [bar]	1.4
Hub/tip diameter [mm]	660/800
Pressure ratio (1st Stage, total-to-total)	1.35
Blade Count	
Stator 1	36
Rotor	54
Stator 2	45

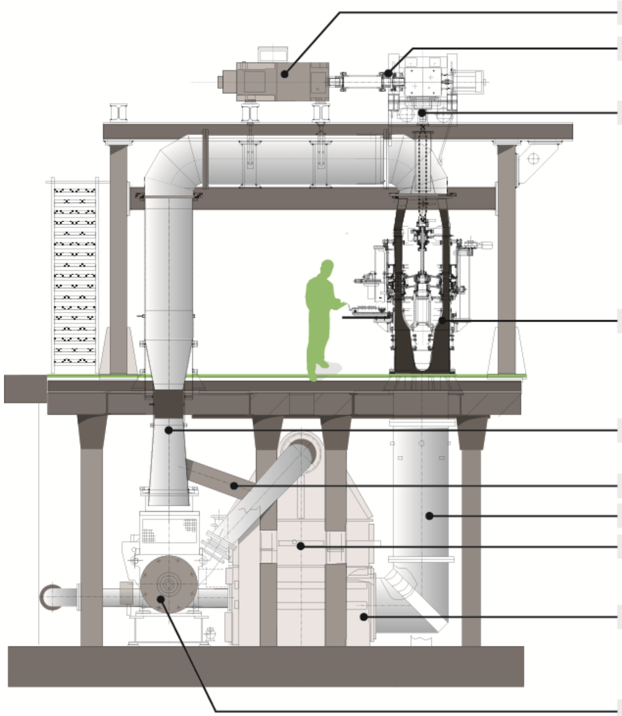

Time-Resolved Area Measurements at Stator 1 exit

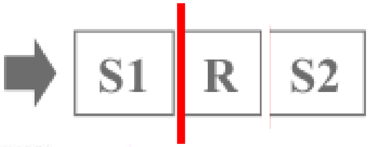

Total Pressure [Pa]

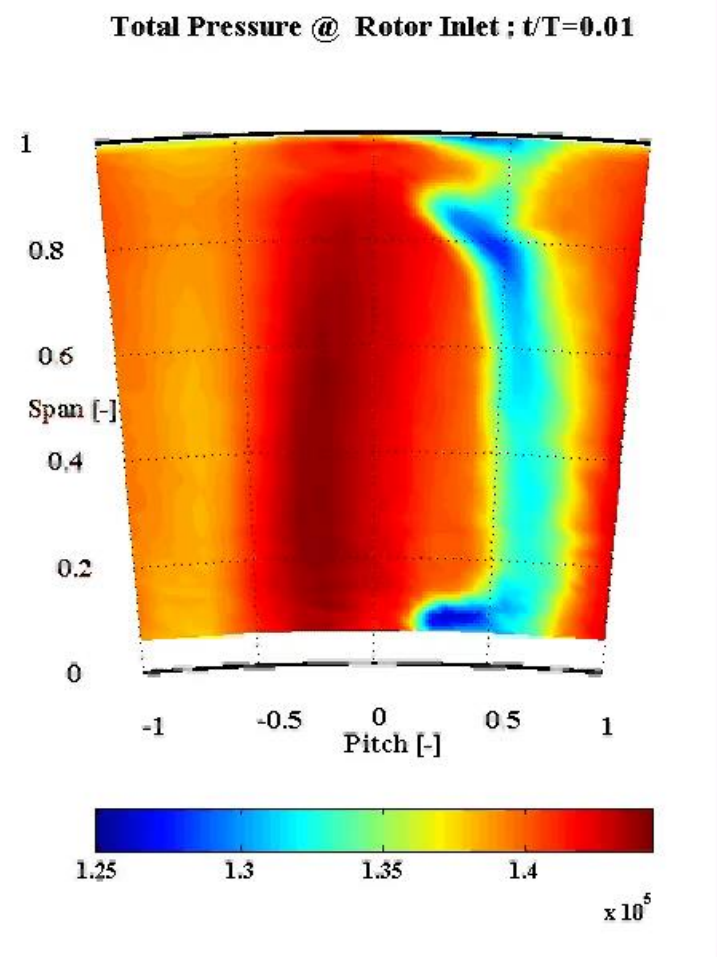

Yaw Angle [Deg.]

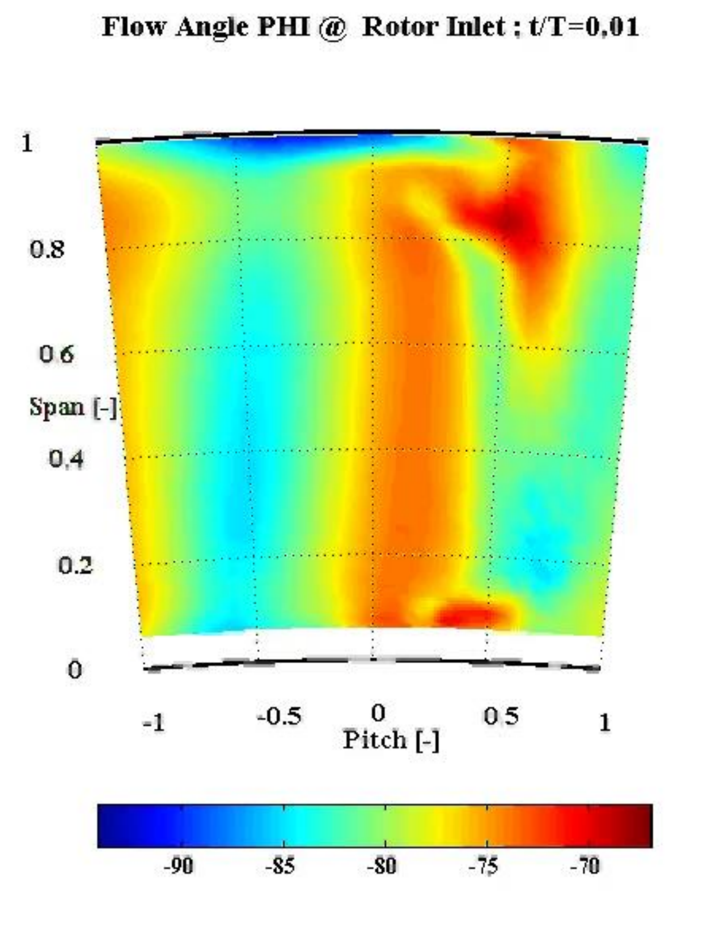

Time-Resolved Area Measurements at Rotor Exit exit

Total Pressure Coefficient [-] over 2 Stator2 pitches

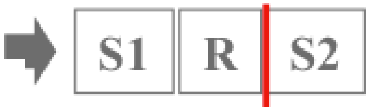

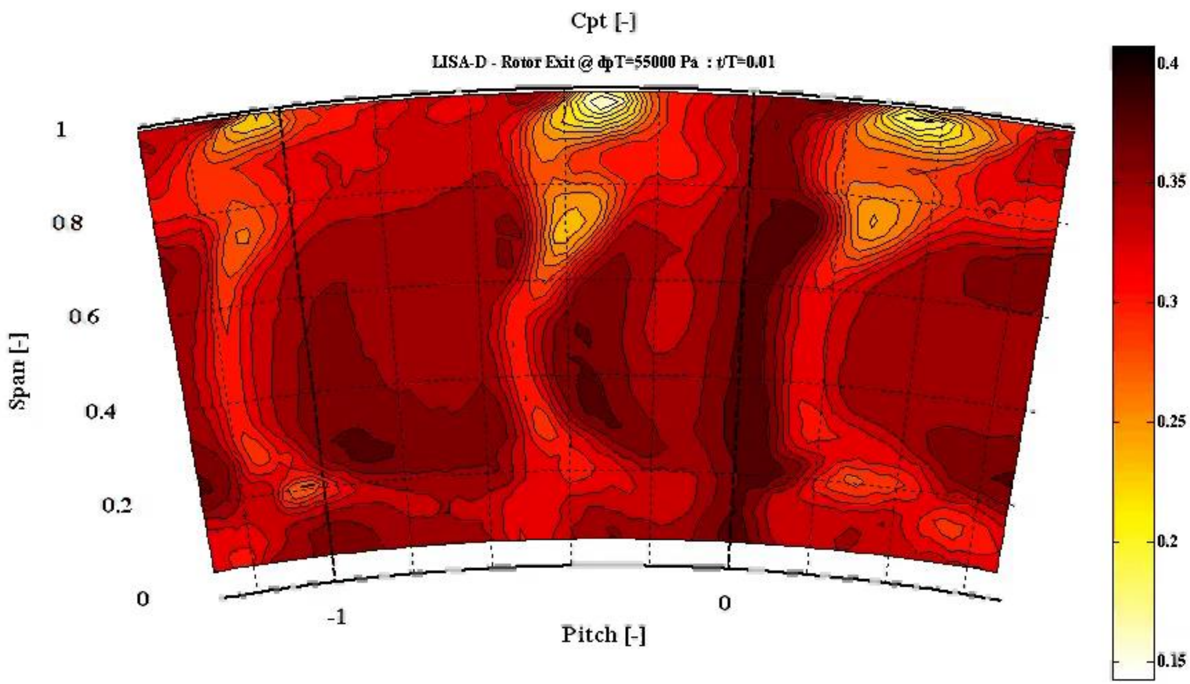

Time-Resolved Area Measurements at Rotor Exit exit

Total Pressure [Pa]

P'$_0$ RMS [pa] Level of stochastic total pressure fluctuation

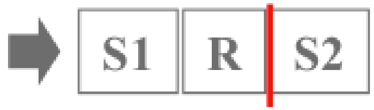

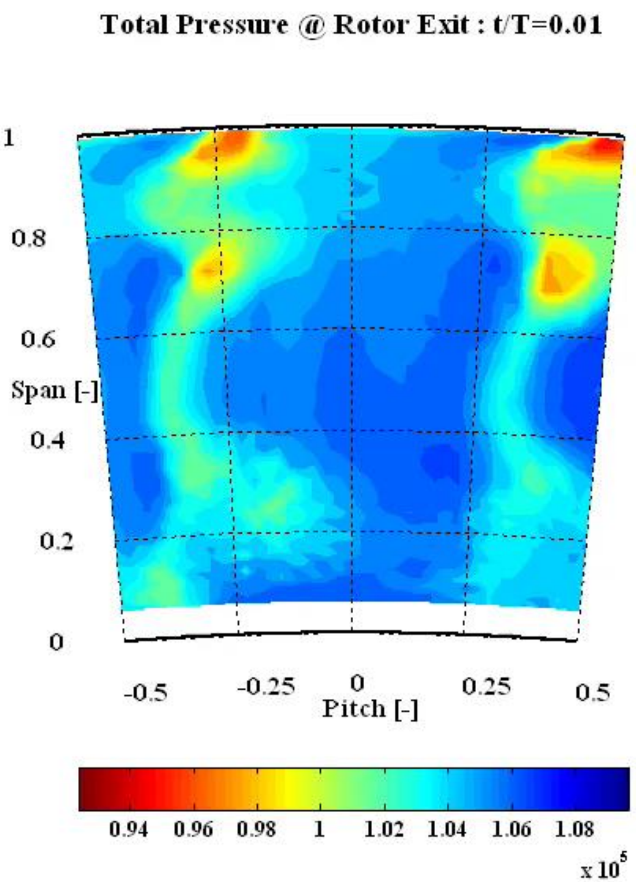

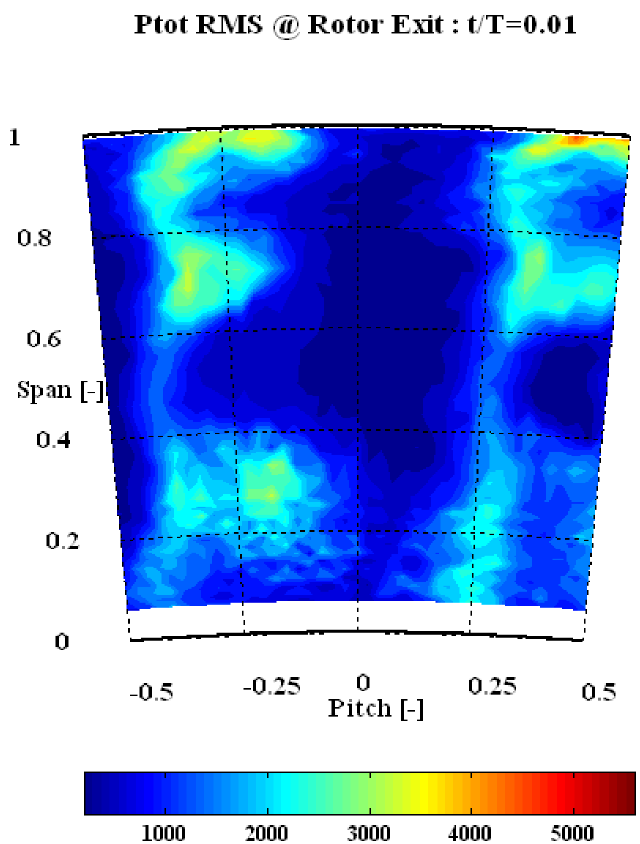

$$P'_{(t)} = P_{(t),FRAP} - \left(\bar{P}_{(t)} + \tilde{P}_{(t)}\right)$$

- 1° Total pressure loss correlated to P_0'RMS
- 2° Rotor secondary flow loss modulation due to:
  - 1st stator wake structure
  - 2nd stator potential field

In-House Ultra Miniature Pressure Sensor
& Multi-sensor Telemetry System
for stationary and rotating facilities
超小型 圧力センサー
及び マルチセンサー用 テレメトリー システム
静止体／回転体用

In-House Ultra Miniature Pressure Sensor: Application

- In the early stage of new turbine or compressor development, the design focuses on satisfying the **mechanical integrity of the rotating parts** to meet the requirements in terms of expected effective operating hours. -> **nearly 30% of the development cost**

- it is vitally important to study the sources of **inter-blade row interactions** on the aerodynamic blade excitation to **mitigate the risk of early failure**.

- It requires conducting **measurement in the rotating frame of reference**, which is more challenging to construct and instrument at the same degree than stationary experiments.

Packaged Pressure Transducer

- **Flush-mounted assemblies:**
  - Ultra miniature:1.75 x 0.81 x 0.47mm Al container -> **smallest on market**
  - Connected through 75μm thick flexible circuit, length: 20mm – 250mm, **high measurement density, installation onto 3D surfaces**
  - Absolute pressure range: 0 – 2bar
  - Temperature range: 10 – 120° C
  - Measurement bandwidth = 210kHz
  - **Tested up to 50'000g**
- **Operates in air and steam**
- **Calibrated against pressure and temperature**

Flush-mounted

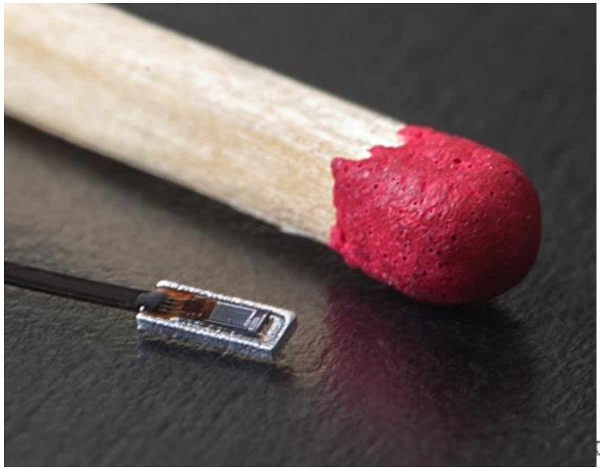

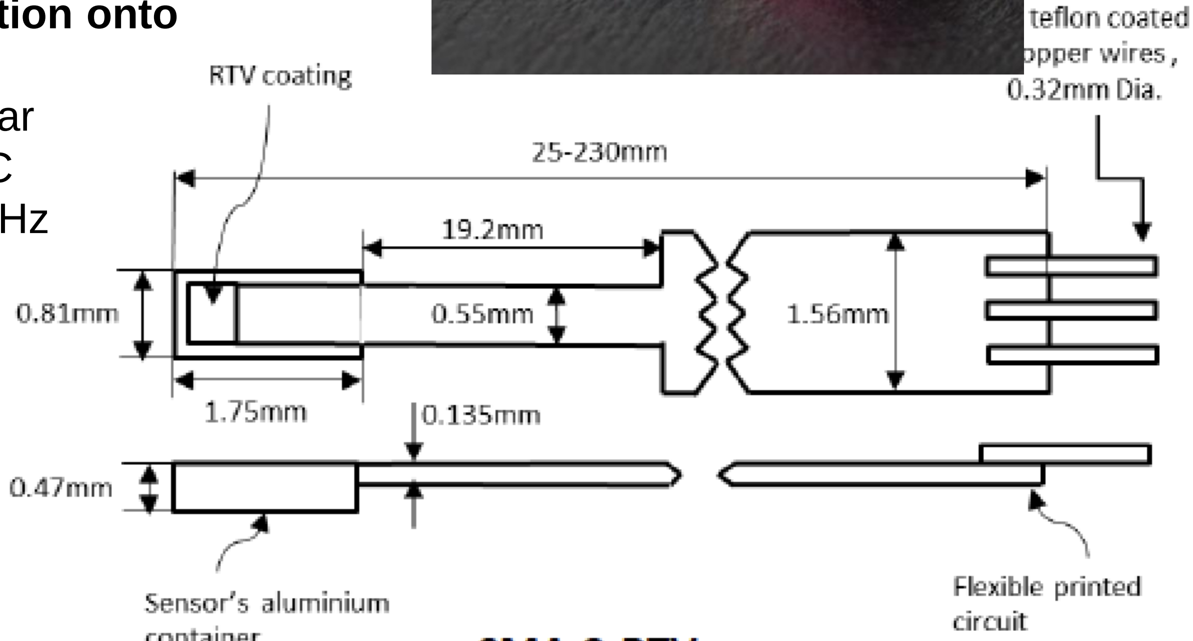

SMA-2-RTV

Wireless Data Acquisition System

- Signal Conditioning and data acquisition
  - Diameter: 64.9mm / height: 9mm
  - Built-in current source: 0.25 to 10mA
  - **4 AI channels(simultaneous) / 7 DIO**
  - 0-5V analogue input
  - **2-stage variable gains with intermediate voltage offset**
  - **16bit resolution**
  - **200 KHz sampling rate**
  - **On-board storage (8GB μSD card)**
- **Simultaneous measurements** of more than **16 boards** through **synchronization with optical trigger -> 64 channels synch.**
- **Board control and data download through WiFi**
- Compatible with**: pt100, strain gages, piezo-resistive pressure sensor**

Top/Bottom view

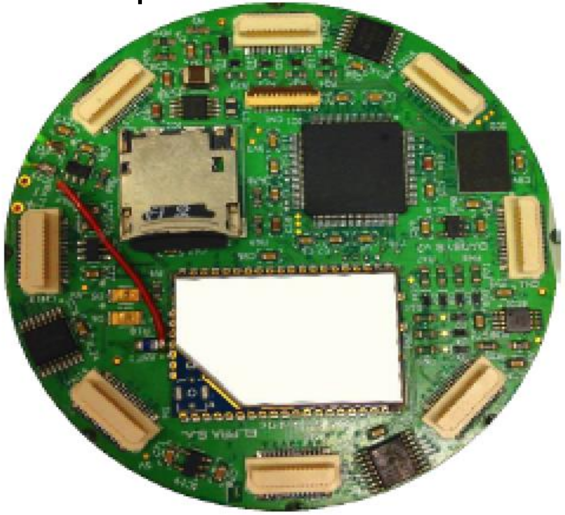

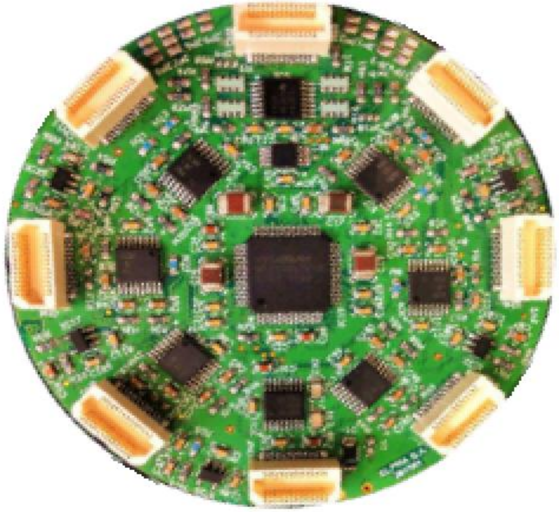

Unsteady Loading Axial Turbine

- In LEC 1-1/2 stage axial turbine LISA
- 16 sensors @ 25% span + 16 sensors @ 85% span on rotor blade
- WiFi DAQ boards on rotor disk at 132mm off-center axis and powered through slip-ring

Rotor speed [RPM]	2700
Pressure ratio (1.5-Stage, total-to-static)	1.60
Turbine entry temperature [°C]	55
Total inlet pressure [bar]	1.4
Hub/tip diameter [mm]	660/800
Pressure ratio (1st Stage, total-to-total)	1.35
Blade Count	
Stator 1	36
Rotor	54
Stator 2	45

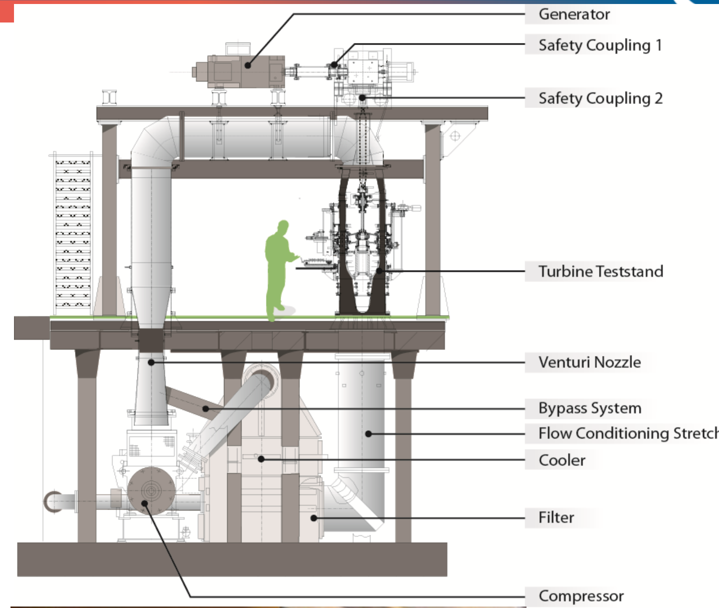

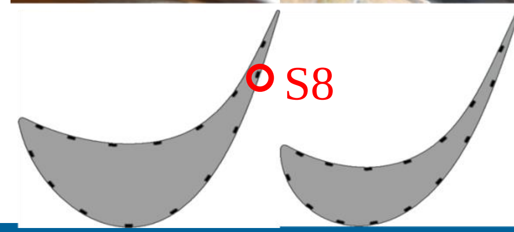

Unsteady Loading Axial Turbine

Time-resolved surface pressure measurements at 25% span on rotor shows:

- Periodical impingement of NGV1 wake main source of surface pressure fluctuation on suction side of rotor leading edge
- Surface pressure on suction side of rotor trailing affected by superposition of several frequencies
- Blade surface unsteady pressure peak-to-peak fluctuation on rotor trailing edge 25% higher than at leading edge
- System provides up to 6pa unsteady pressure measurement resolution

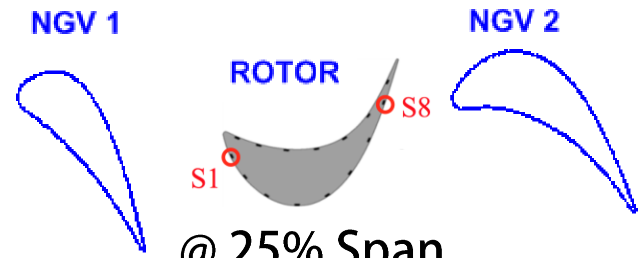

@ 25% Span

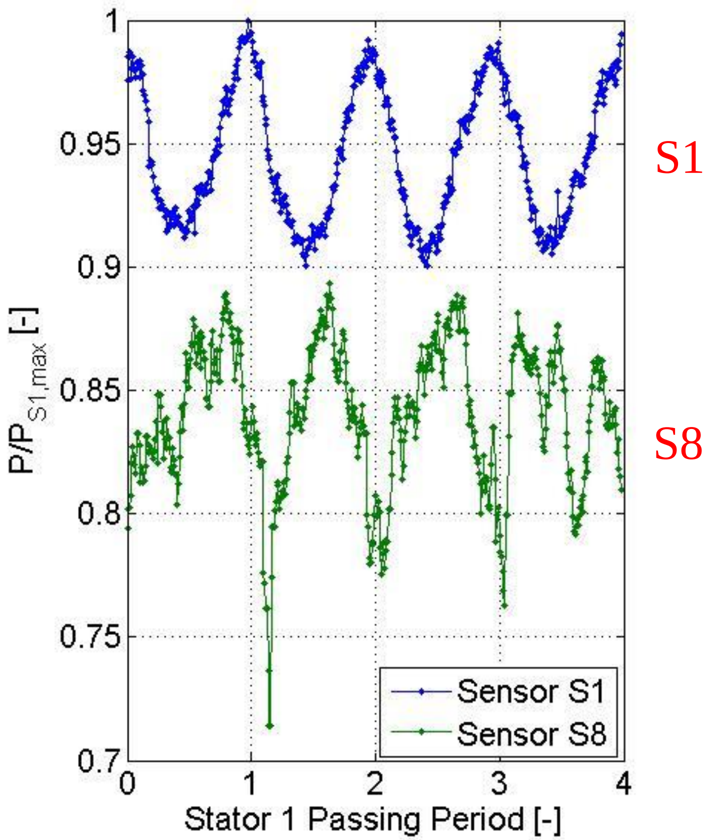

Unsteady Loading Axial Turbine

At 25% span of rotor suction side, surface pressure affected by presence of rotor hub passage vortex interacting (intensity & position) with:

- NGV1 wake (1620Hz) @ -0.35 pitch
- NGV 2 potential field (2025Hz) @ 0 pitch
- 2st harmonic of NGV1 (4860Hz)

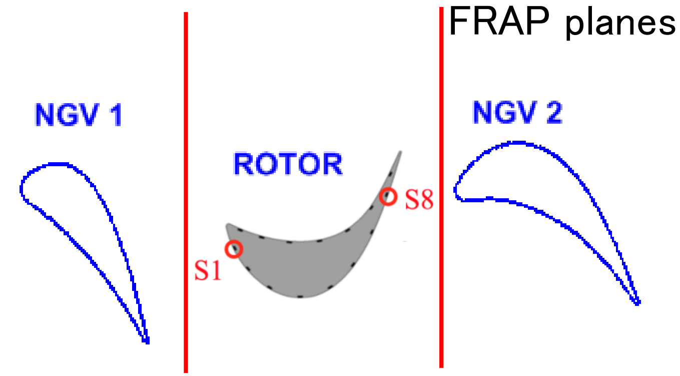

Rotor Inlet/Outlet Total Pressure Fluctuation

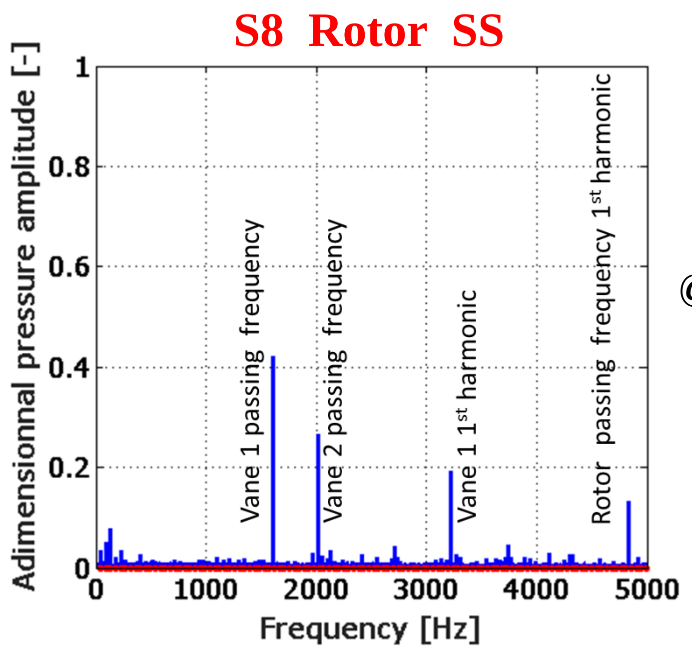

@ 25% Span

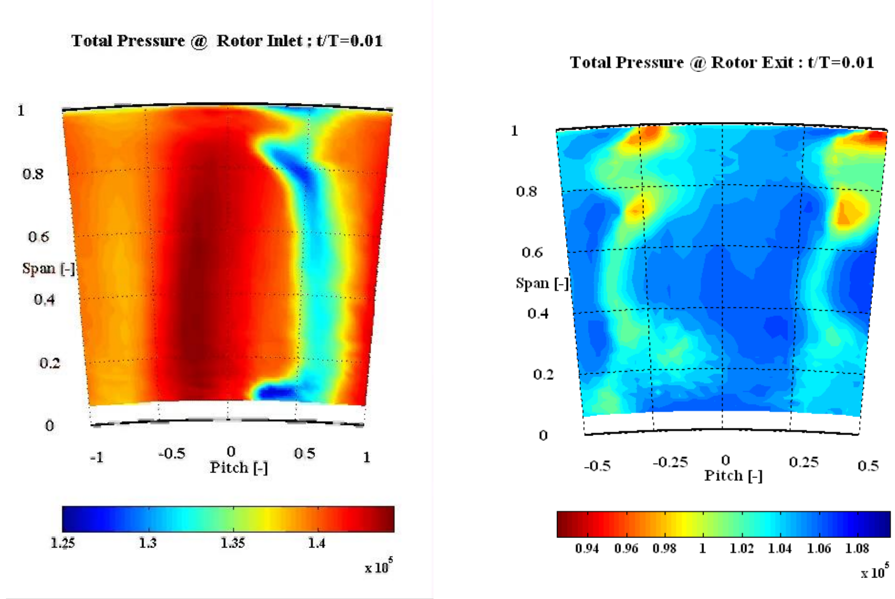

Flush-Mounted Pressure: Impeller Blade Forced Response Equipped with Varialble IGVs

Pressure Sensor Packaging

Electrical leads (75µm Flexible printed circuit)

Bonded sensor into container (RTV coated or with «pepper pot» screen)

Instrumented Impeller

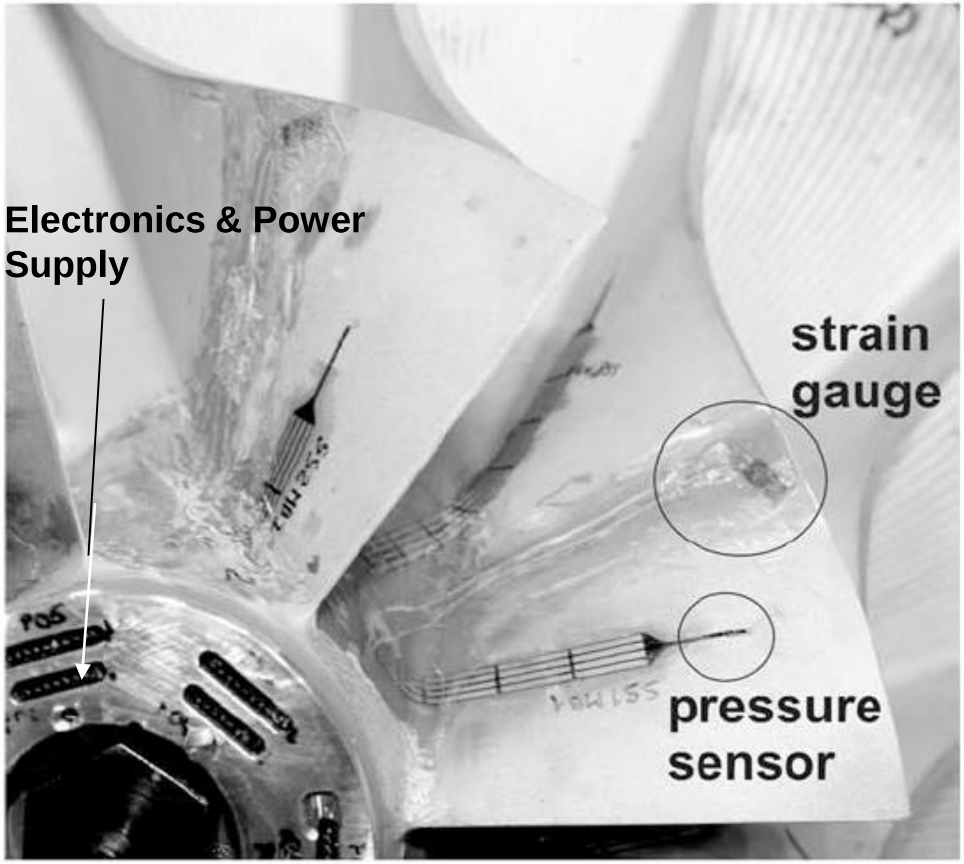

Flush-Mounted Pressure: Impeller Blade Forced Response Equipped with Varialble IGVs

Embedded on-board electronics

- Aerodynamically shaped
- Cooling system
- System acquisition triggered through optical laser
- Powered through battery pack

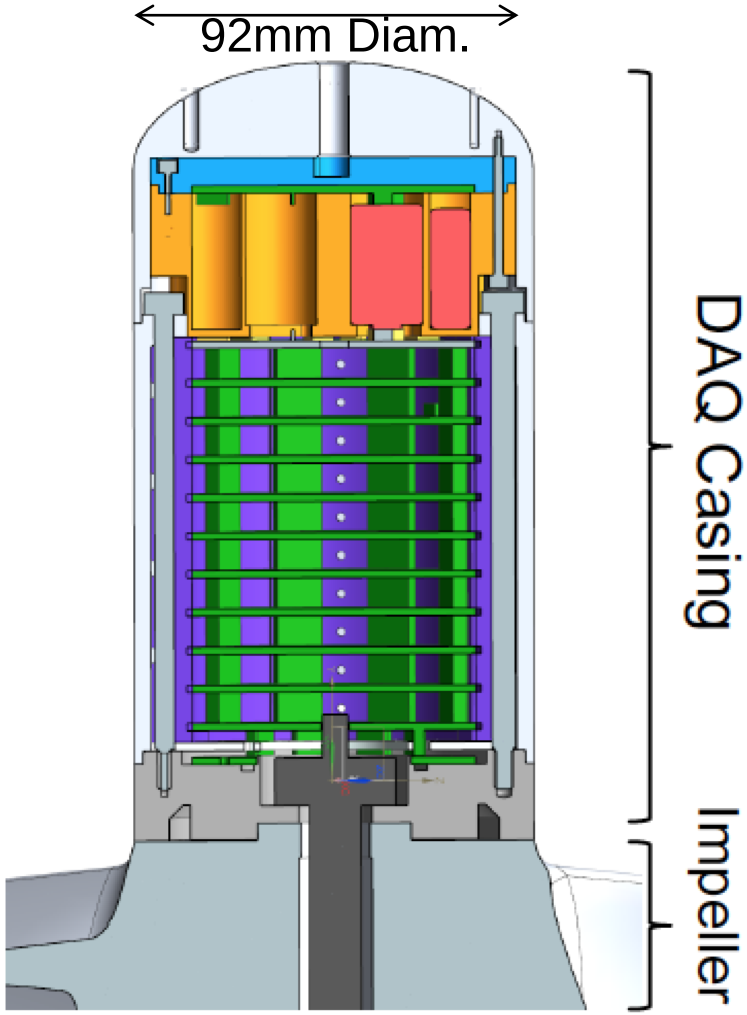

Flush-Mounted Pressure: Impeller Blade Forced Response Equipped with Varialble IGVs

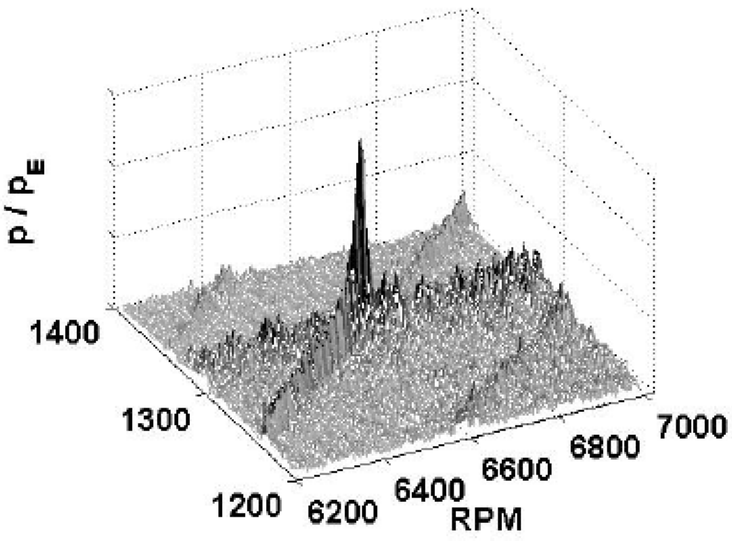

(a) Pressure Sensor Response

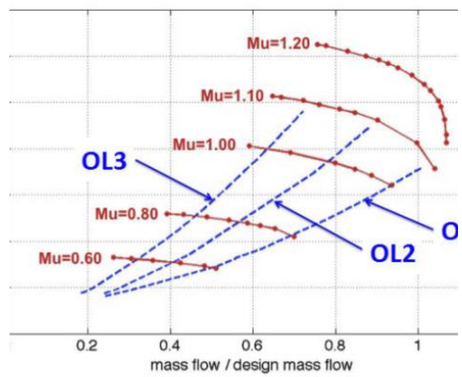

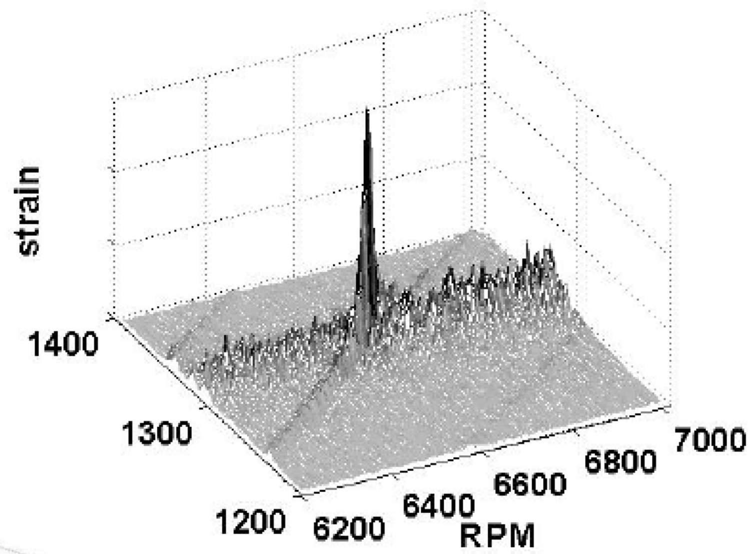

(b) Strain Gauge Response

- Effect of inlet flow distortion on blade excitation
- Correlation of pressure and displacement
- Derive blade unsteady forcing and aerodynamic work distribution

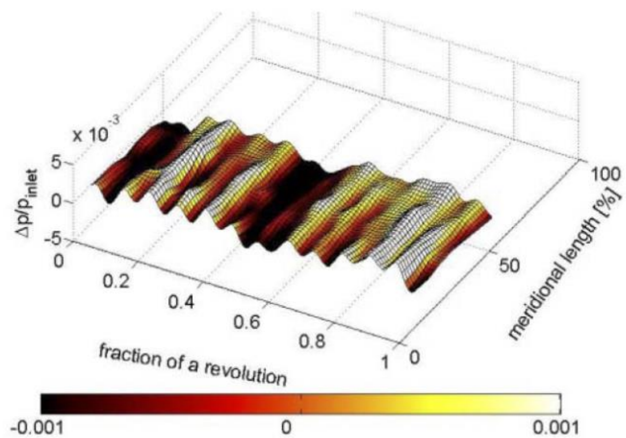

FIGURE 9. Measured Unsteady Blade Pressure Fluctuation $\Delta p'_{PS-SS}$ at Mid-Span, 0° *IGV* at *OL2*

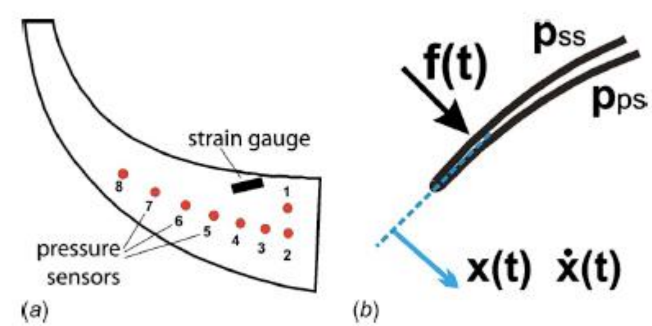

Casing Mounted Fast-Pressure Sensors: Application

- **Turbine hub cavities modes** provoke highly unsteady flow structures which are characterized by **low frequency, non-synchronous pressure fluctuations -> source of HCF, loss aerodynamic**

- **Tip leakage flow study**

- **Time resolved static pressure at casing wall**

Packaged Pressure Transducer

- **Wide range of packaging size (customized)**
- **Wall-mounted assemblies**
  - Smooth or threaded housing (4mm in Diam. or M6)
  - RTV coated or with protective screen on sensor
  - Reference back pressure tube
  - Absolute Pressure range: 0 – 2bar (can be extended to 12bar)
  - Differential pressure range: ±1bar
  - Temperature range: 10 – 220° C
  - Measurement bandwidth: up to 250kHz
- **Operates in air, steam or water**
- **Calibrated against pressure and temperature**

Wall-mounted

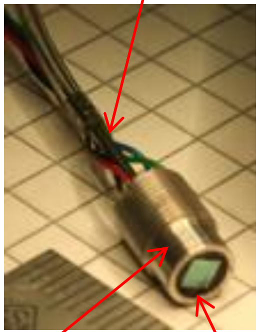

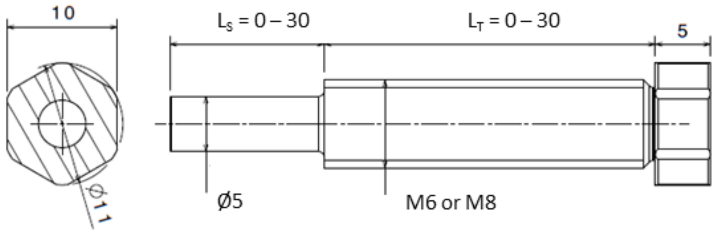

Dimensions in mm

Modulation of Turbine Hub Cavity Mode by Rim Seal Purge Flow

- Turbine configuration and blading:
  - 1.5 — stage configuration (S1 / R / S2)
  - Blade count: S1: 36 / R: 54 / S2: 36
  - Unshrouded rotor with cylindrical end walls
  - HP gas turbine blading: $\psi = 2.34,\ \phi = 0.57$

- Rim seal purge flow injection:
  - Off-take from primary air loop
  - Injection into Stator1-Rotor hub cavity
  - Rim seal purge flow injection rate:

$$IR = \frac{\dot{m}_B - \dot{m}_S}{\dot{m}_{Main}} \cdot 100\ (\pm 0.01\%)$$

  - Measured operating conditions at design point: IR0=0.0%, IR1=0.4%, IR2=0.8%, IR3=1.2%

Schematic purge flow path

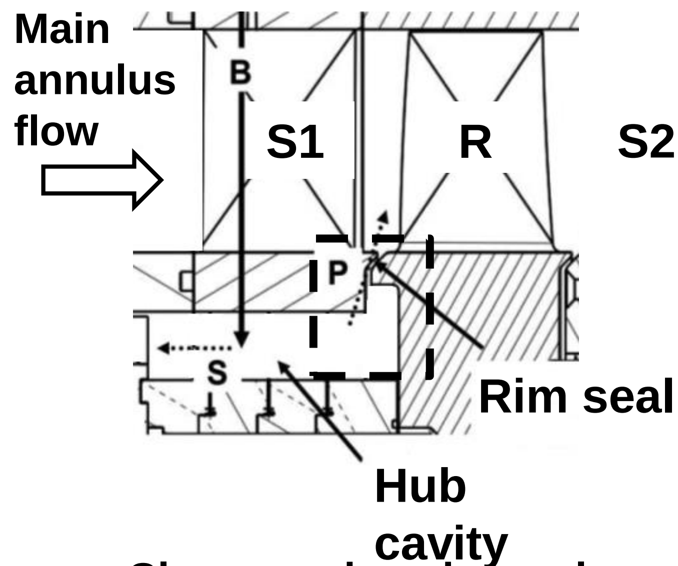

Close-up view rim seal

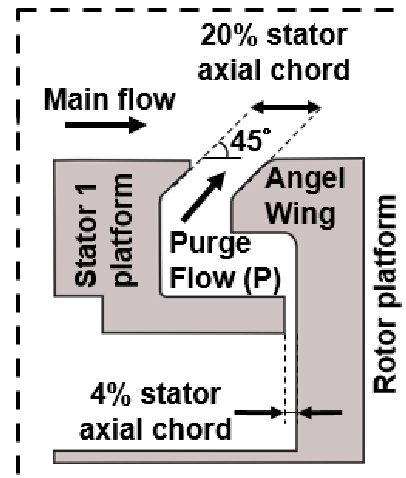

Source of cavity modes: rotating low static pressure zones (CFD)

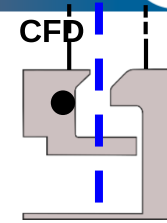

- **Low static pressure zones observed, which are:**
  - Rotating with the rotor at a fraction of the rotor speed
  - Sensitive in number and rotational speed to purge flow

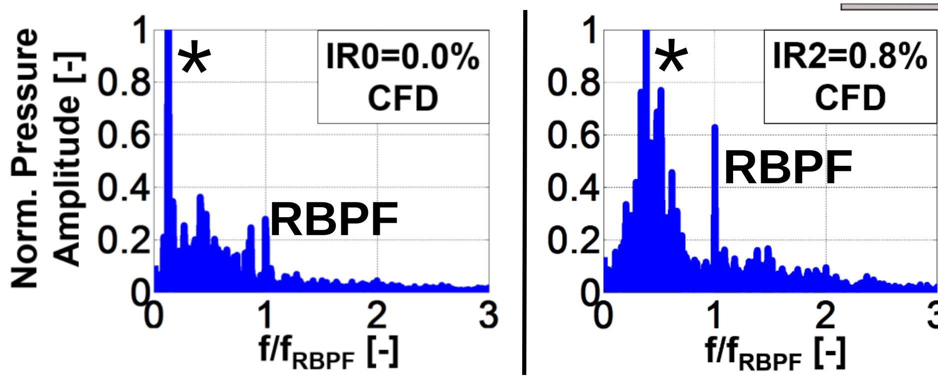

- **Band of low frequencies (*) captured by CFD**

IR	0.0%	0.8%
f/f_{RBPF} (CFD)	13-20%	27-51%
f/f_{RBPF} (EXP)	13-20%	25-35%

- **Number of zones x rotational speed equals the cavity mode frequencies**

Maps of instantaneous static pressure

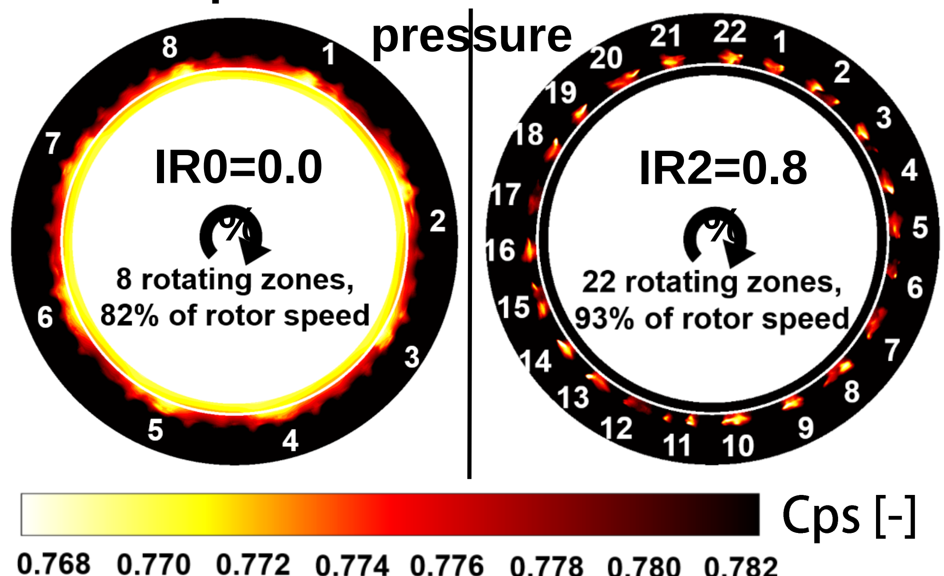

Cavity modes show strong sensitivity to purge flow

Hub cavity sensors

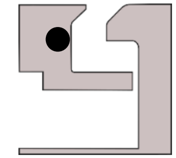

- Band of low frequencies with elevated pressure amplitudes in hub cavity: cavity modes

- Frequency shift for increasing purge flow:

IR	0.0%	0.4%	0.8%
f/f_{RBPF}	13-20%	21-26%	25-35%

- Pressure amplitude changes with purge flow:
  - IR1=0.4%: 2x higher amplitudes compared to RBPF

- Cavity modes are suppressed for high purge flow rates IR3=1.2%

Hub cavity pressure frequency

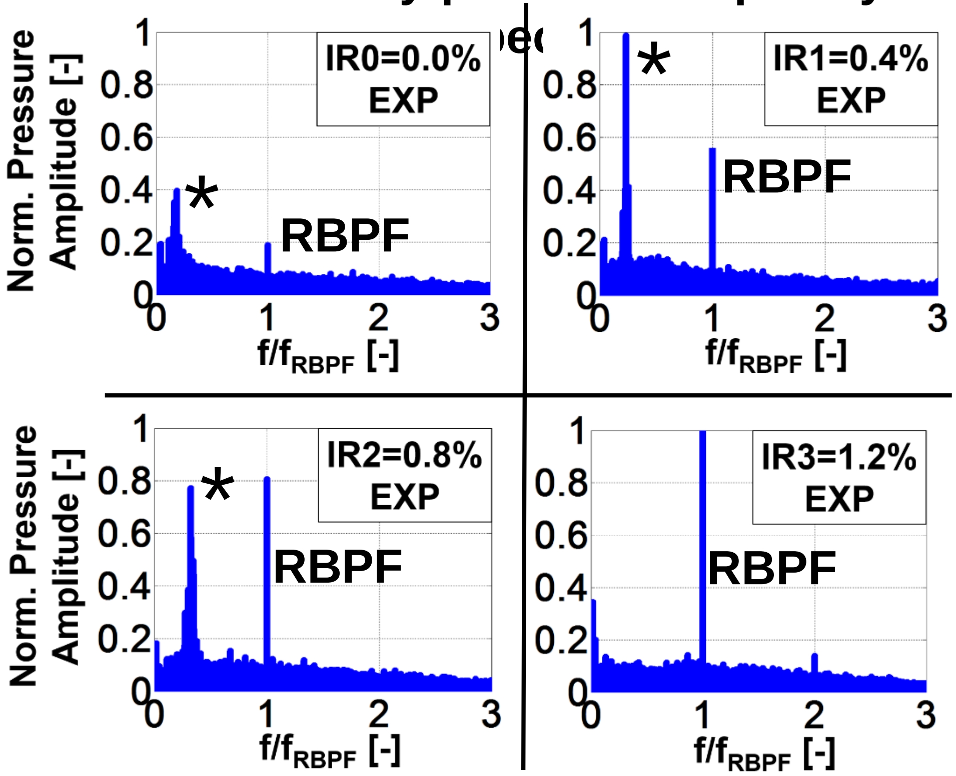

* Low frequency cavity modes

RBPF: Rotor blade passing frequency

Substantial increase in noise due to cavity modes

Hub cavity sensors

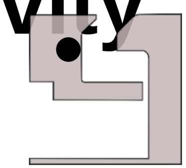

- Low frequency pressure fluctuations are in **human perception of sound**
- **Pressure amplitude change** due to different purge flow is transferred into **different noise levels at the source**
- **Peak level of noise emission** is reached at **moderate purge flow rate IR1=0.4%**: **+18dB** relative to suppressed IR3=1.2%
- **Noise characteristic** of turbine hub cavity **changes with purge flow rate**

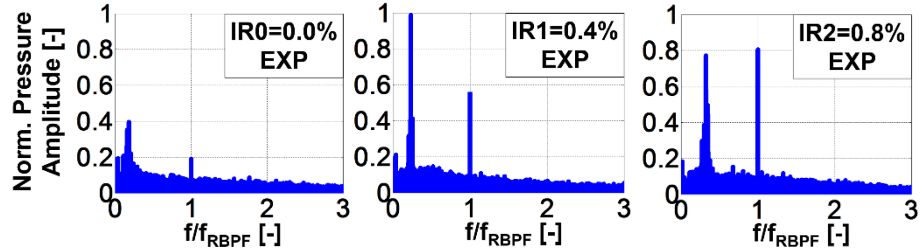

Increase in noise vs. purge flow rate dependent cavity modes

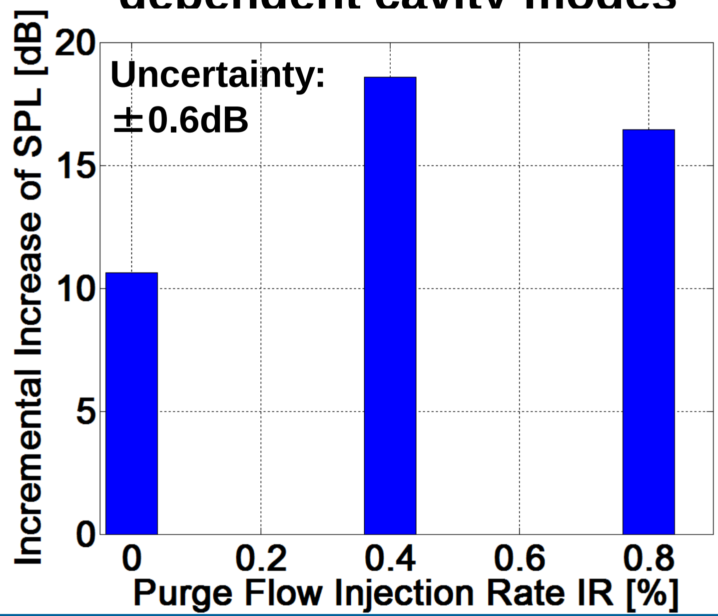

Instrumentation for Wet Steam and Particle Laden Flows
ウエット蒸気 及び 粒子含有流体用 計装

Motivation

- Introduction of renewables into the electricity grid
  - Variability in power generation
  - Difficult to predict
  - Steam turbines require operational flexibility (60% of entire generated electricity power production worldwide)
  - Efficient and safe operation during part load conditions (LSB)

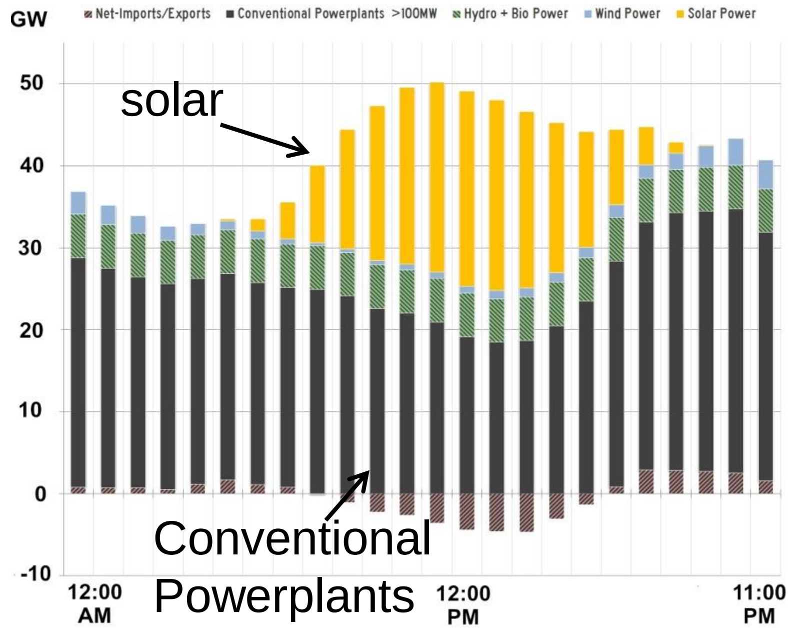

Germany's electricity production in a hot day

Fast response probe for wet steam flow field measurements (FRAP-HT Heated)

- 2.5 mm tip diameter
- Two piezo-resistive silicon pressure transducers encapsulated under shielded pressure taps for direct droplet impact protection
- Measurement bandwidth 25 kHz
- High power density miniature heater ($61 W/cm^2$)
- to 8% of wetness mass fractions and Ma=0.7
- Probe tip is heated above steam flow saturation temperature to keep pressure taps unclogged
- Provide: yaw, pitch, P_{stat}, P_{tot}

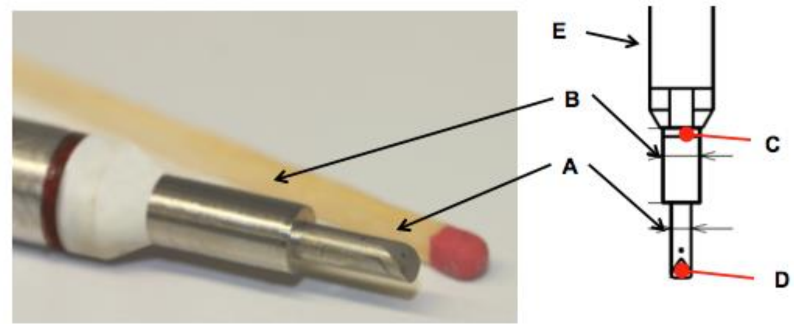

A...Probe tip (Diameter: 2.5mm)
B…Heating elements (Diameter: 4.7mm)
C…Heater temperature monitoring
D…Tip temperature monitoring

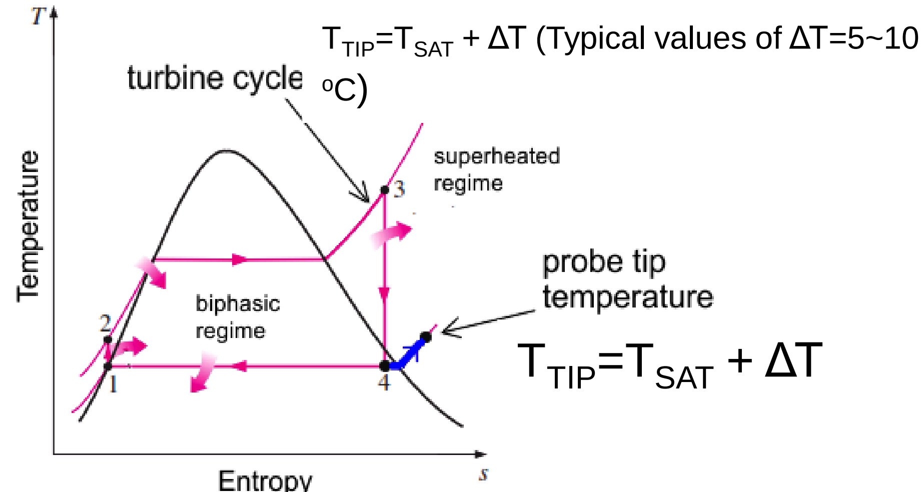

Operating principle of the miniature heater

- High power density miniature heater consists of high specific resistance heating wire installed in a double helix spiral (cancels the AC electromagnetic noise)
- Probe tip sensors' temperature are controlled using closed loop PID regulator
- Pressure sensors' temperature is used for the feedback loop control
- Tests showed that the heater:
    1. Has no effect on measured flow quantities
    2. Aero-calibration coefficients deviation below 1%

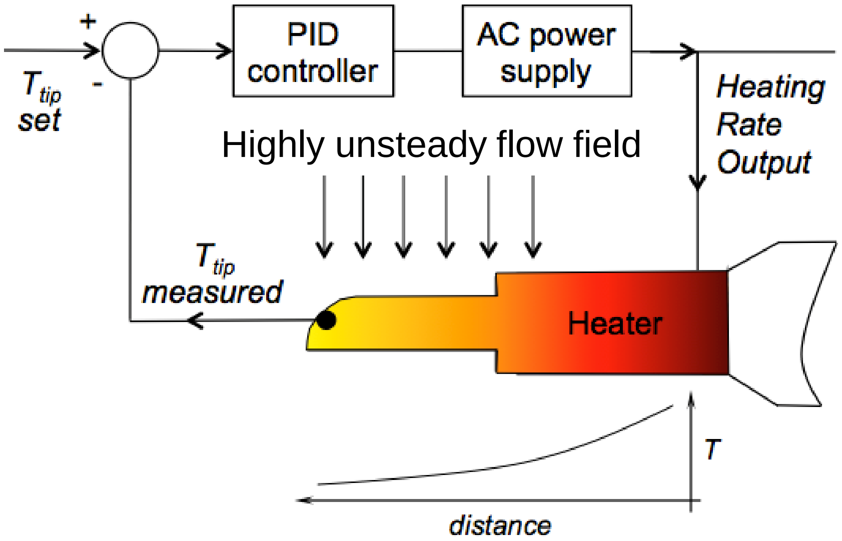

FRAP-HTH Extended Aerodynamic for High Flair Angle Turbines

Coefficients for $P_1 \geq P_4$ (Blue sector)	Coefficients for $P_4 \geq P_1$ (Red sector)
$K_\phi = \frac{P_2 - P_3}{P_1 - \frac{P_2+P_3}{2}}$	$K_\phi = \frac{P_5 - P_6}{P_4 - \frac{P_5+P_6}{2}}$
$K_\phi = \frac{P_1 - P_4}{P_1 - \frac{P_2+P_3}{2}}$	$K_\phi = \frac{P_4 - P_1}{P_4 - \frac{P_5+P_6}{2}}$
$K_\phi = \frac{P_{tot} - P_1}{P_1 - \frac{P_2+P_3}{2}}$	$K_\phi = \frac{P_{tot} - P_4}{P_4 - \frac{P_5+P_6}{2}}$
$K_\phi = \frac{P_{tot} - P_{stat}}{P_1 - \frac{P_2+P_3}{2}}$	$K_\phi = \frac{P_{tot} - P_{stat}}{P_4 - \frac{P_5+P_6}{2}}$

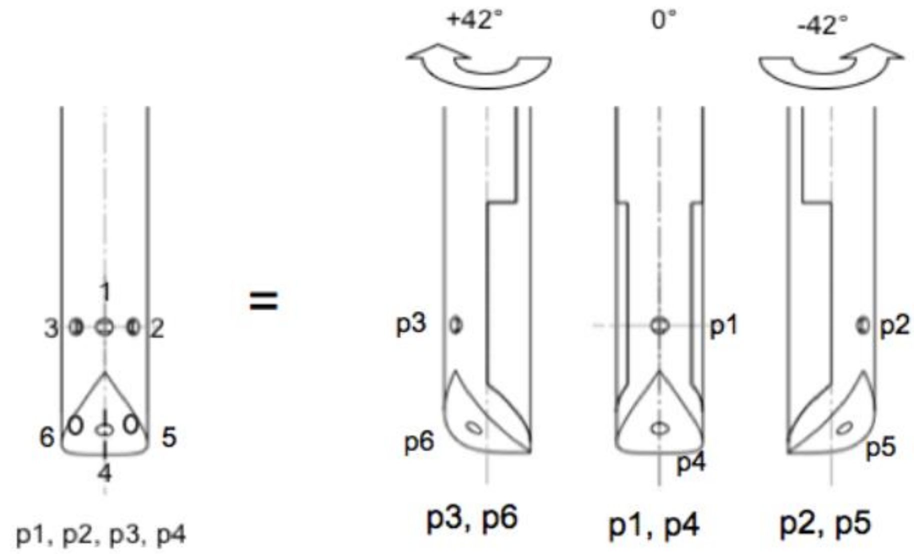

Measurement concept in virtual 6-Hole mode with 2-Hole probe

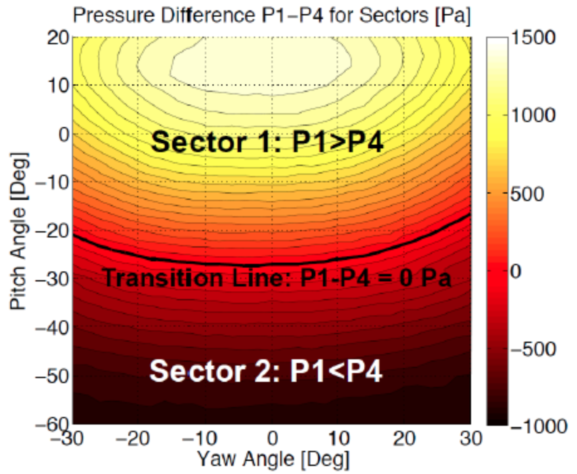

Virtual 6-sensor concept with extended pitch measurement range calibration in Freejet facility:

- 60° < pitch < +20
- -30° < yaw < +30°

Experimental research facility — investigation of part load conditions

Industrial LP steam turbine test facility

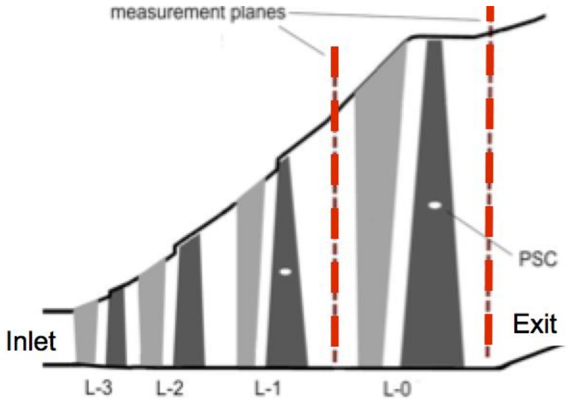

Measured Unsteady Total Pressure
LP steam turbine exit
Span vs. Time

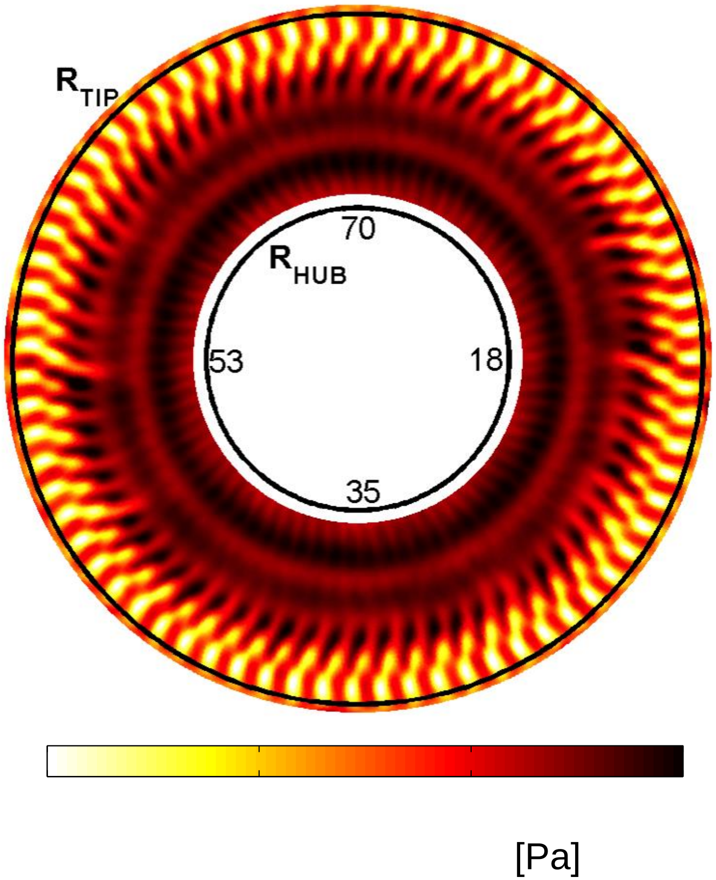

	High load	Part load
Massflow		77%
Exit Pressure [kPa]	8.0	8.0
Inlet Temperature [^oC]	272	272
Wetness L-0 [%]	8.0	6.5

Single traverse measurement developed against time

Time-averaged measurements 5HP Vs. FRAP-HTH

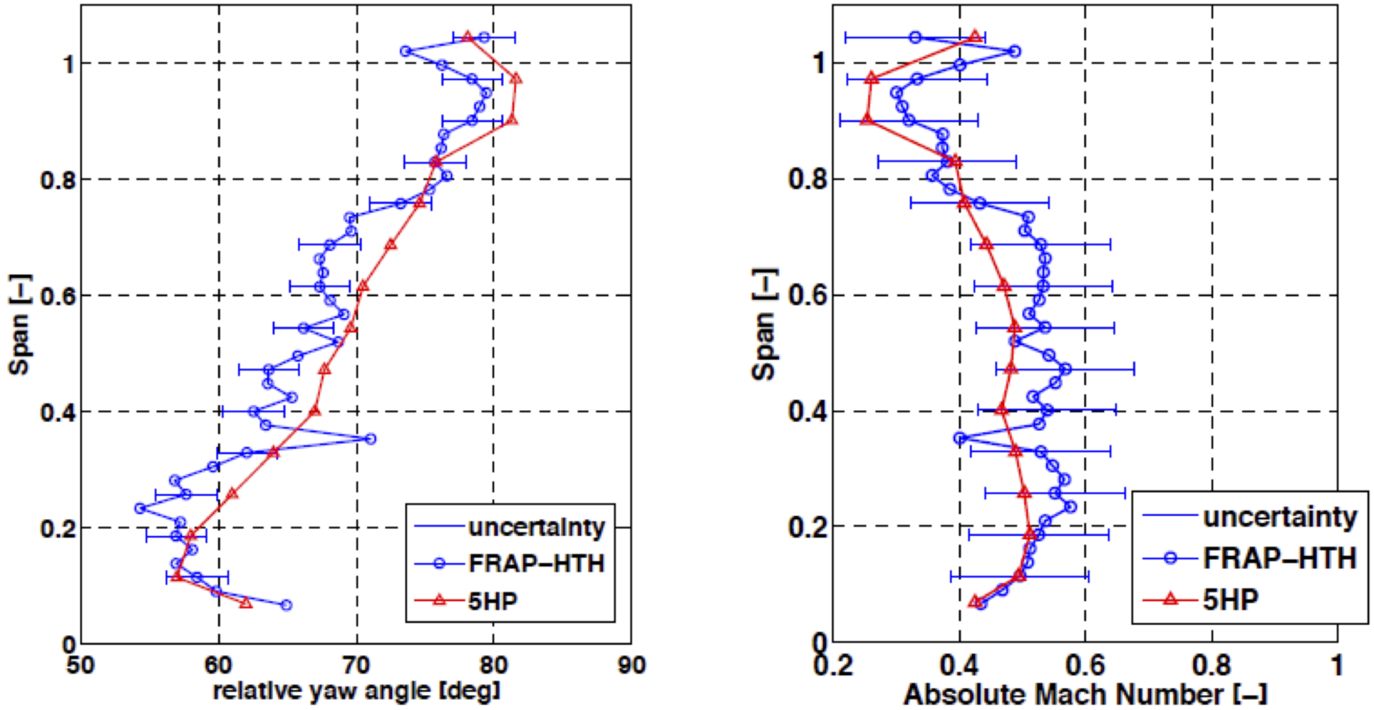

- 8% wetness mass fraction @ L–0 exit
- Good agreement despite different upstream stator clocking position
- Within measurement uncertainty bandwidth

Radial velocity distribution: Flow redirection towards blade tip

- Time averaged radial velocity results show:
  - High Load: Vradial≈0   up to 85% span
  - Part Load: Vradial>>0 up to 85% span
- Low reaction zone is affected (hub)
  - Negative incidence angle
  - Small separation at the blade hub
- Flow is redirected towards the blade tip region when the mass flow is reduced by 23%

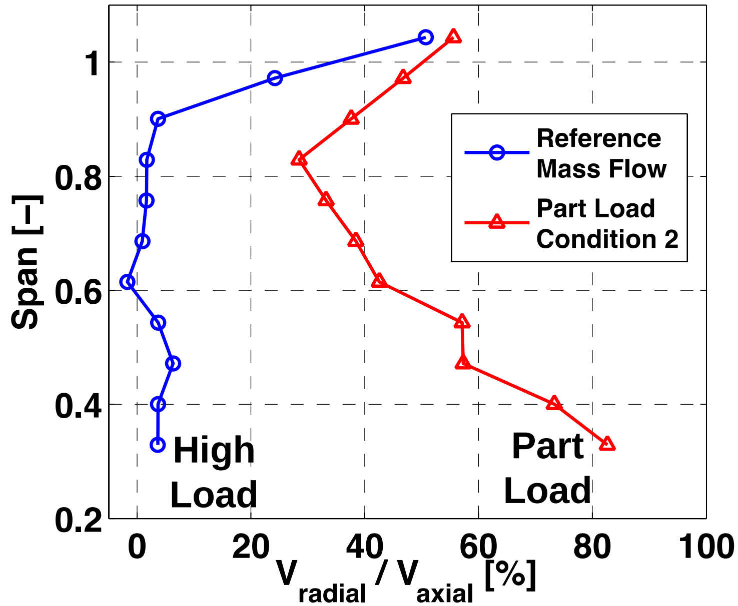

Time averaged **Radial Velocity** for:
High Mass flow &
Reduced Mass flow by 23%

Part load condition shows increase in intensity of secondary flow structures

1. Several turbulent flow structures can be identified between 80 to 100% span for both cases
2. Secondary flow features at part load condition (80–95% span) exhibit higher levels of stochastic unsteadiness:
   - 60% larger for the structures at 95% span
   - 25% larger for the structures at 80% span

$$Ptot_{(t)}' = P_{FRAP,(t)} - (\bar{P}_{(t)} + \tilde{P}_{(t)})$$

Stochastic unsteadiness

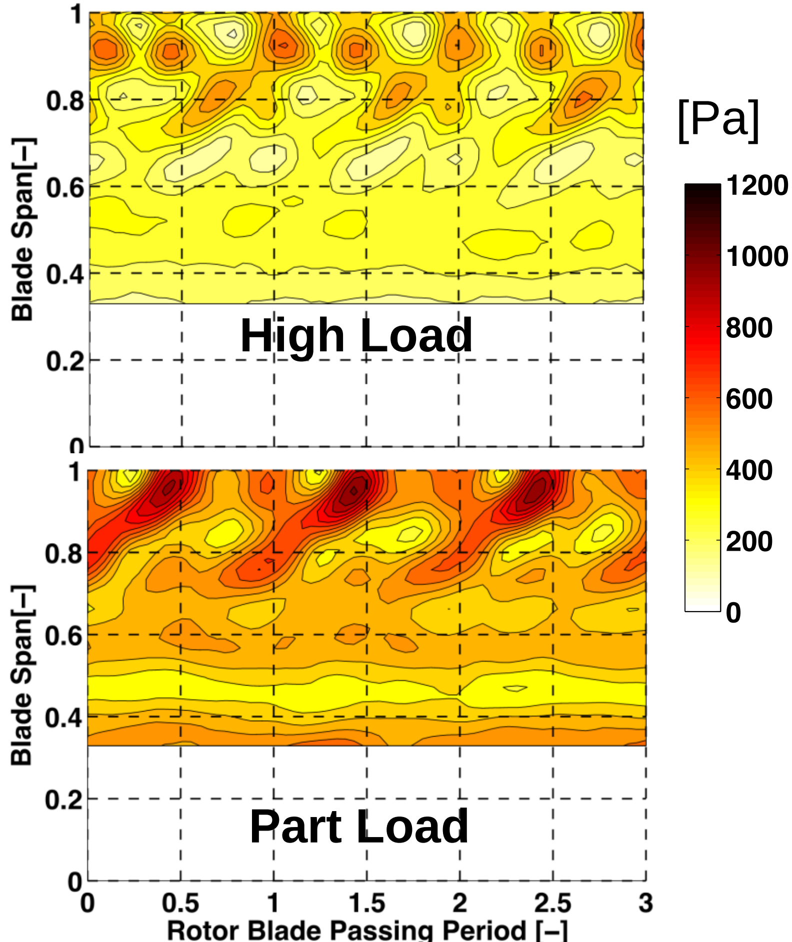

FRAP-HT Heated Applied in LP Steam turbine (stage L-0)

P'_o RMS [pa] $Cp_{o,rel}$ [pa]

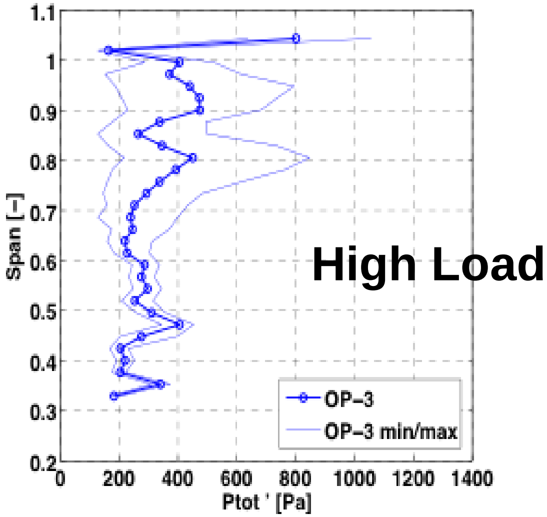

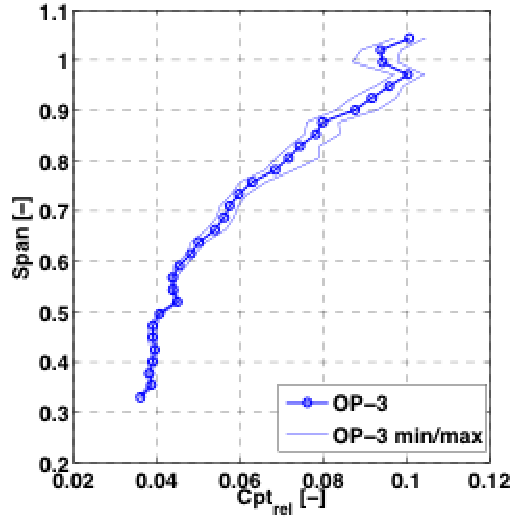

@ L-0 :

- Enables study of time resovled flowfield under various part load conditions
- Decrease of massflow results in:
  - Increase in total pressure loss (+8%) and unsteadiness between 80 and 100% Span
  - Increased turbulence (+52%)
  - Increase of relative total pressure unsteadiness (+28%)

-24% in massflow compared to OP-3

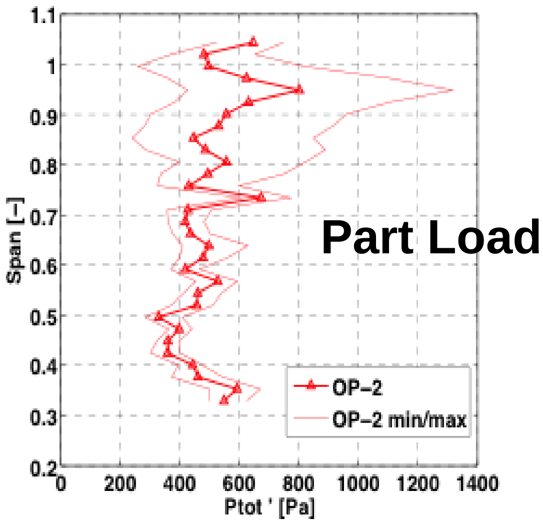

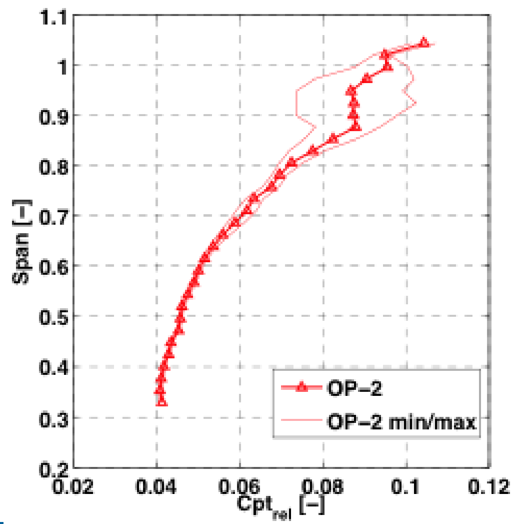

Experimental research facility — investigation of relative supersonic flow conditions at blade tip

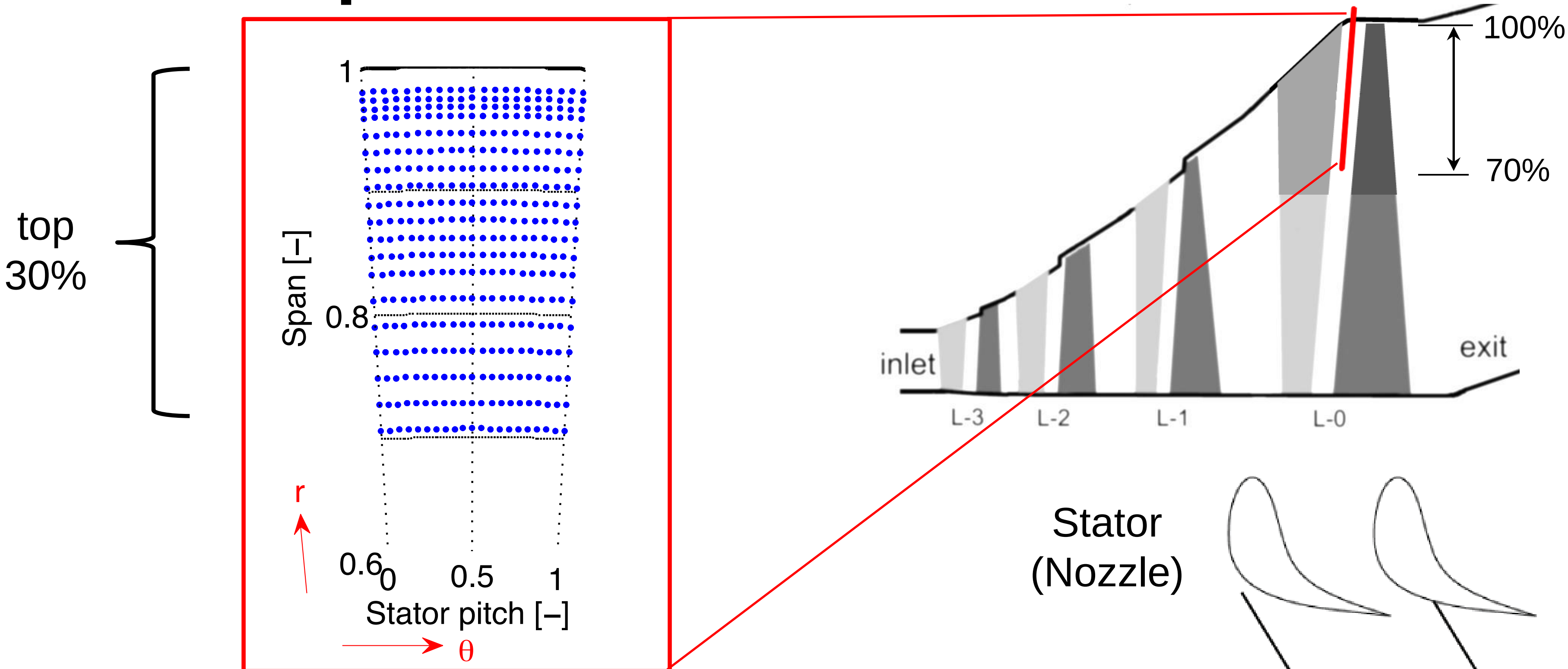

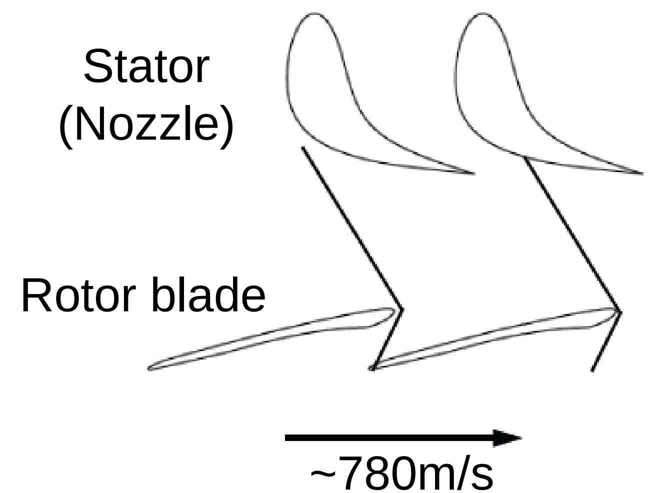

- Probe traverses radially and circumferentially (19 radial points x 21 circumferential traverses)
- Investigate the interblade row interaction of the last stage

Experimental research facility — overview

- MHPS research steam turbine test facility at Hitachi city
- Four stage low pressure steam turbine
- Scale ratio of 1/3
- Stage L-0 has supersonic rotor blade profiles near tip with rotational speed of 180 rps
- L-0 stator equipped with water film suction slit on the upper part of the blade

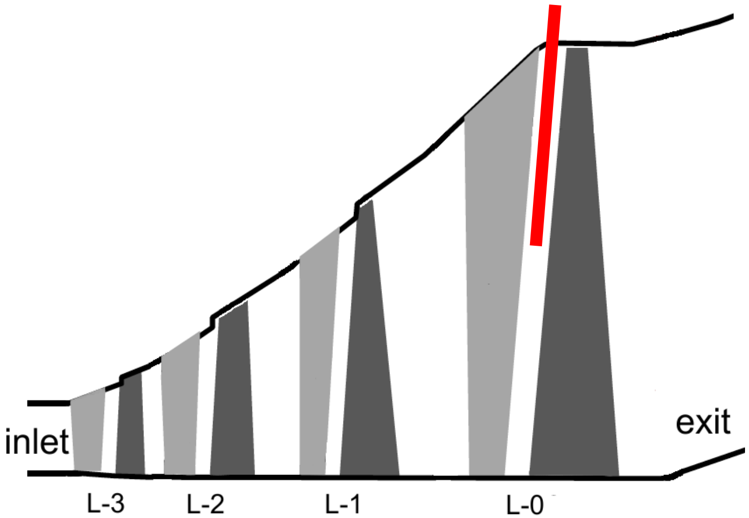

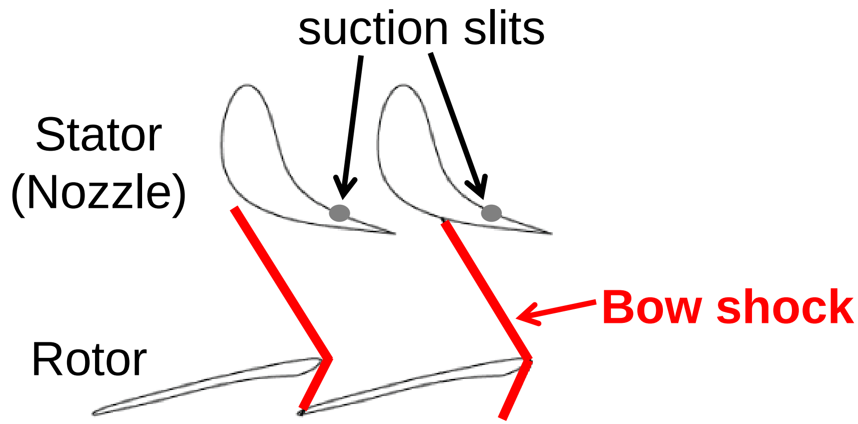

MHPS research steam turbine test facility

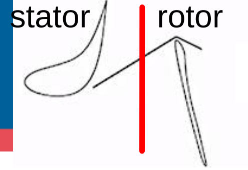

Flow field overview at the stator exit of the last stage

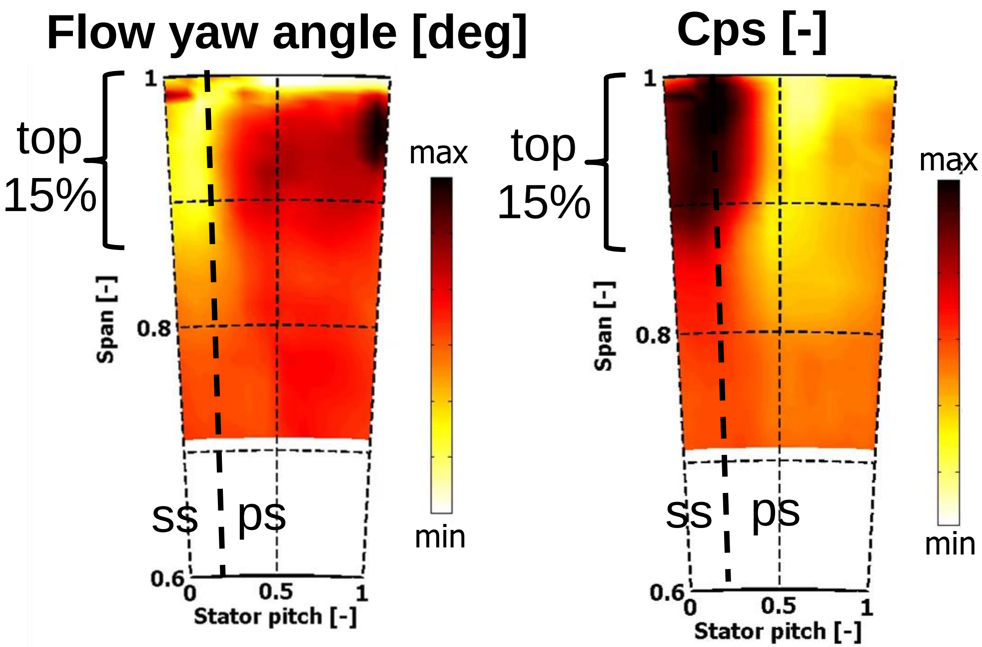

- The flow field is dominated by high unsteadiness at the top 15% of the blade span at the stator exit
- Maximum overturning close to stator wake suction side
- High peak-to-peak fluctuations above 85%. At 90% span:
  - Yaw angle: ±5°
  - Cps: ±30% of the mean value

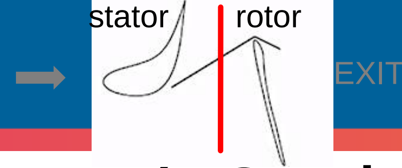

High unsteady values(~3x times) for the top 15% of the blade span

Relative Mach number [-]

Flow yaw angle [deg]

Cps [-]

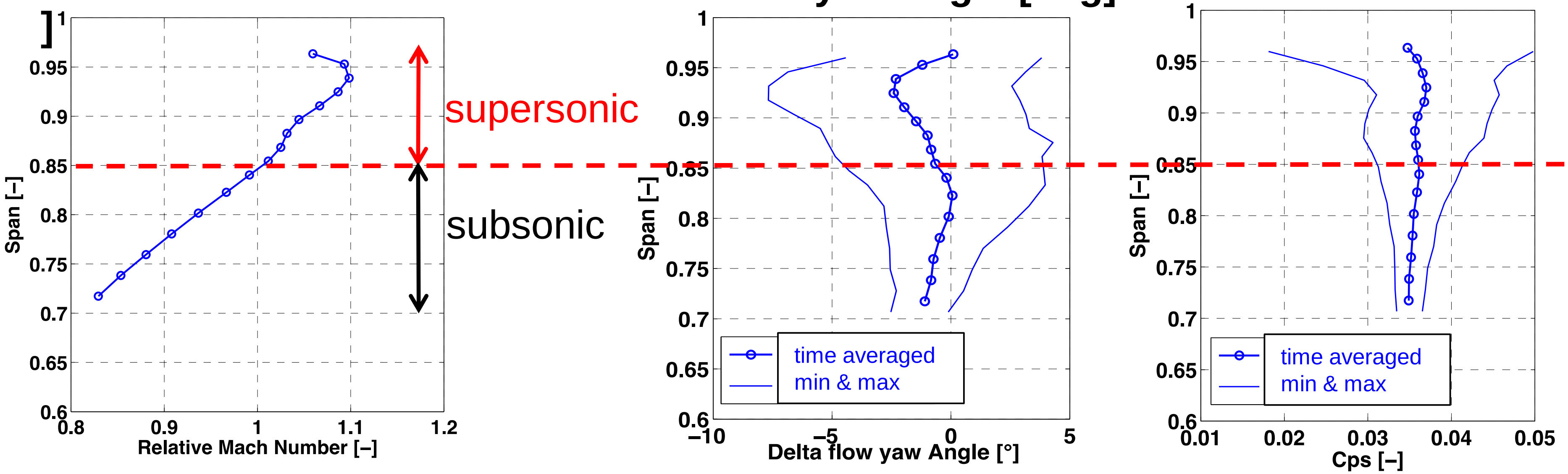

- Supersonic region → span>~85%
- Subsonic region → span<~85%
- Peak-to-peak fluctuations are ~3x times larger on an average in the supersonic region compared to the subsonic region (top 15% of the blade span)

Motivation

- Part load conditions
  - ➢ P_s & T alter→ Steam quality change (droplet size & concentration are affected)
- Size increase of turbine blades
  - ➢ rpm constant (50 or 60Hz)
  - ➢ Blade length → tip speed
  - ➢ Relative droplet impact speed increases
- Accelerated erosion rate from coarse droplets at the last stage
  - ➢ Aerodynamic disturbances
  - ➢ Mechanical integrity

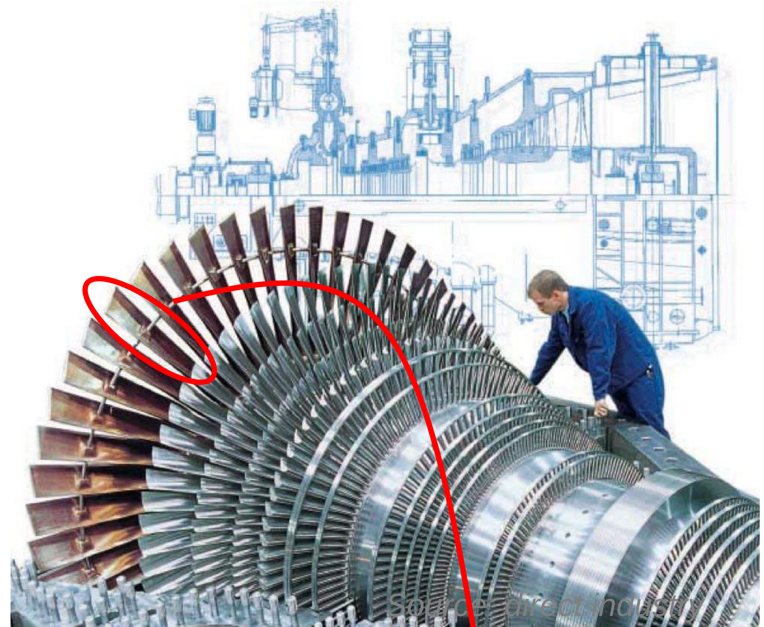

Eroded steam turbine blades (Martinez et al.)

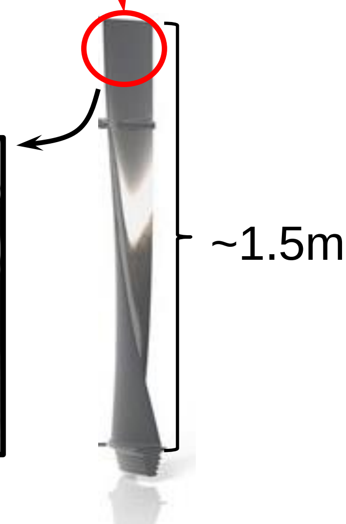

Operating principle: Probe characteristics

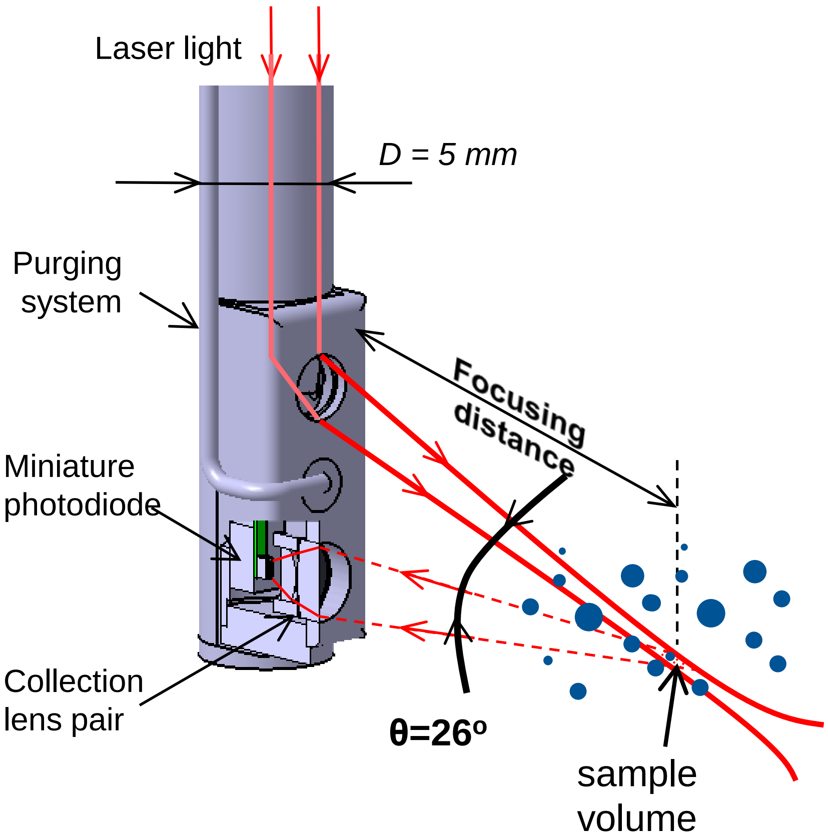

Operating principle and specifications

- Light is guided in the probe tip through an optical fiber
- Set of lenses focuses the beam into sample volume of 0.01mm^3 of 3 x Probe-Diameters
- Set of collecting lenses captures the backscattered light and focuses to a miniature photodiode
- Miniature size (diameter: 5 mm)
- Purge flow for lenses clearance

Probe measures:

- Droplet diameter: 30µm to 110µm

  (Max droplet concentration to avoid more than 5% error due to light beam extinction: 10^{12} droplets/m^3)
- Droplet speed: up to 170m/s (Frequency bandwidth 30 MHz)

FRAP-OB Calibration procedure

- Global characteristics:
  - Monodispersed droplet generator
  - Water droplets of: 37-110 μm (σ:±3 μm)
  - Droplet speed: 4-12 m/s
  - High resolution reference camera
    - 5x optical zoom
    - Pixels: 2452 x 2054
  - Droplet monitoring diode for controlling experiment's stability

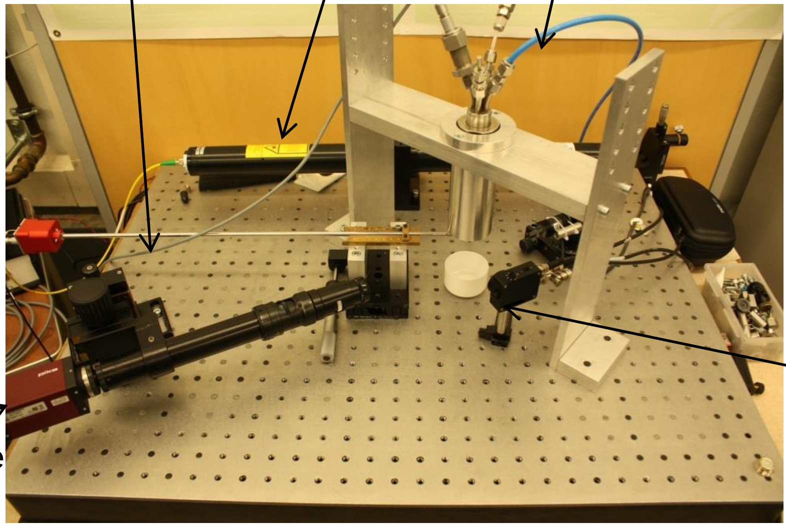

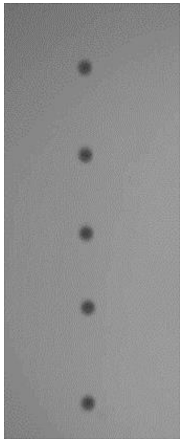

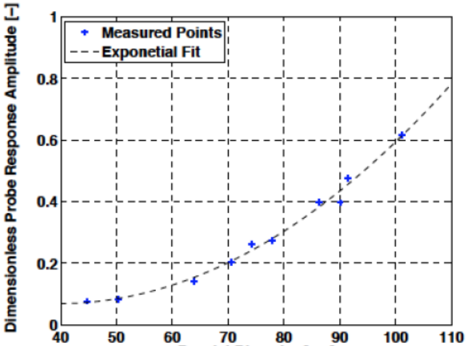

Probe's calibration curve

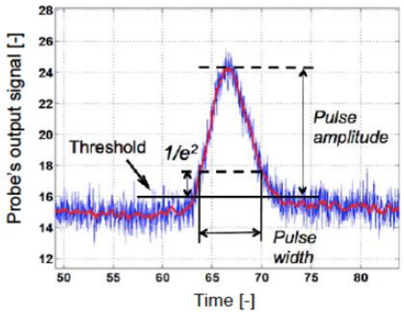

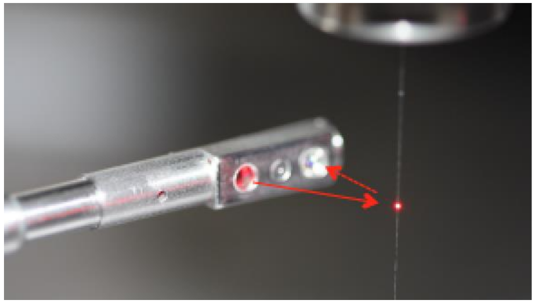

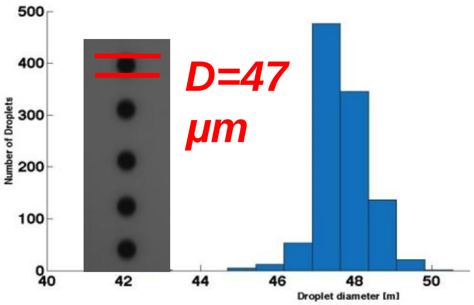

Experimental research facility — overview

- MHPS research steam turbine test facility at Hitachi city
- Four stage low pressure steam turbine
- Scale ratio of 1/3
- Stage L-0 has supersonic rotor blade profiles near tip with rotational speed of 180 rps
- L-0 stator equipped with water film suction slit on the upper part of the blade

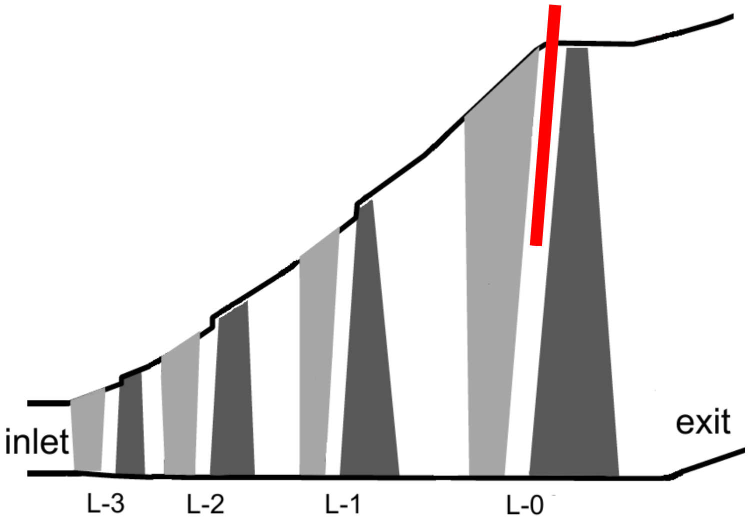

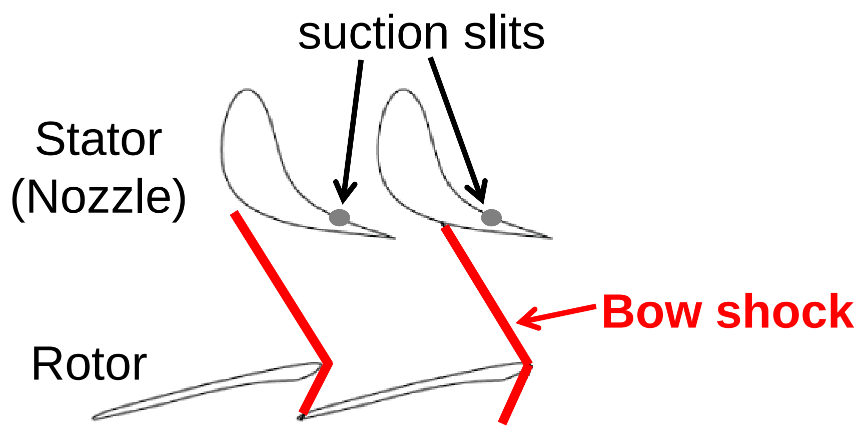

MHPS research steam turbine test facility

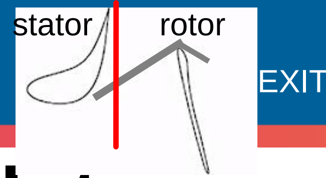

Coarse water droplets present across the entire stator pitch

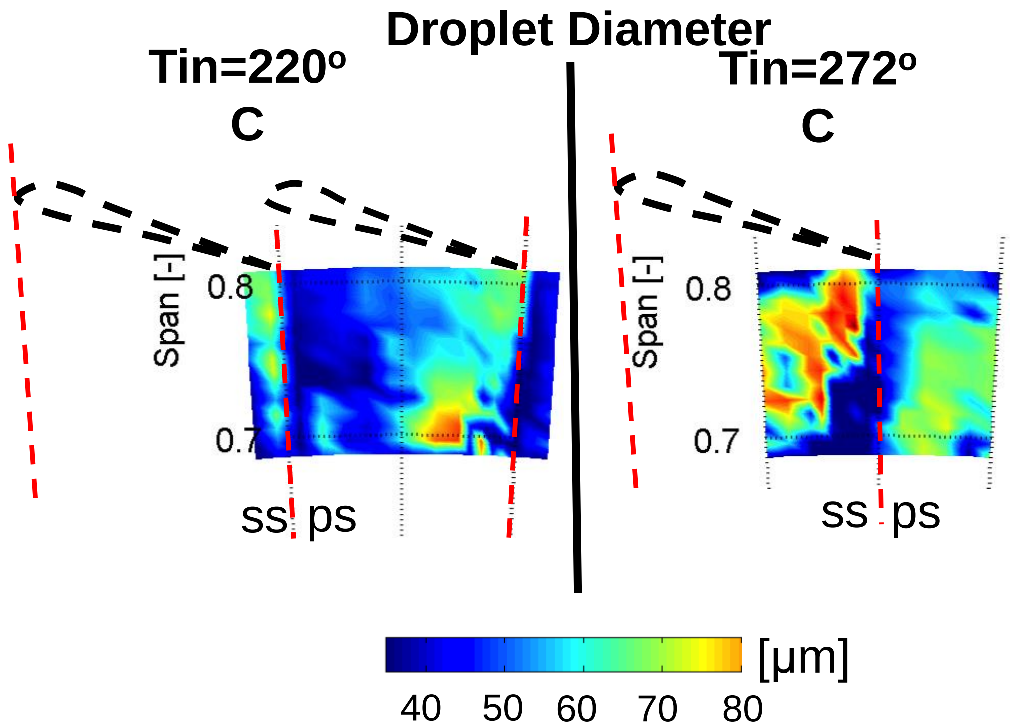

- The measurements over one stator pitch at L–0 stator exit in the top 30% of the blade span
- Results are presented between 68% and 82% span where the measured coarse droplets' count is substantial
- Coarse water droplets:
  1. Present in the entire stator pitch
  2. Size: 37 to 80 μm in Sauter mean diameter between 68–82% span
  3. Large concentration at the vicinity of the stator's suction side for both conditions

Maximum droplet concentration at the vicinity of the stator's suction side

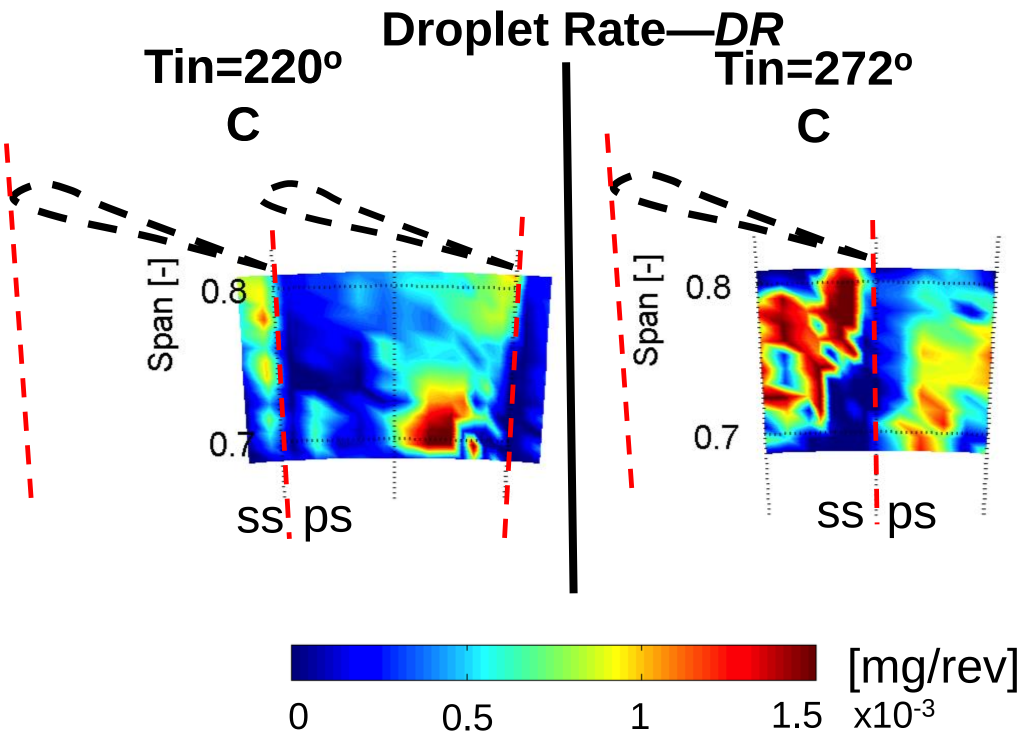

$$DR = \underbrace{N}_{\text{droplet count}}\underbrace{\left(\frac{4}{3}\pi r_d^3 \rho_d\right)}_{\text{droplet mass}}$$

- For both operating conditions the maximum droplet concentration is found to be on the stator's suction side
- The reduced water content on the pressure side can be attributed to the presence of the suction slits

Coarse water droplets formation mechanisms

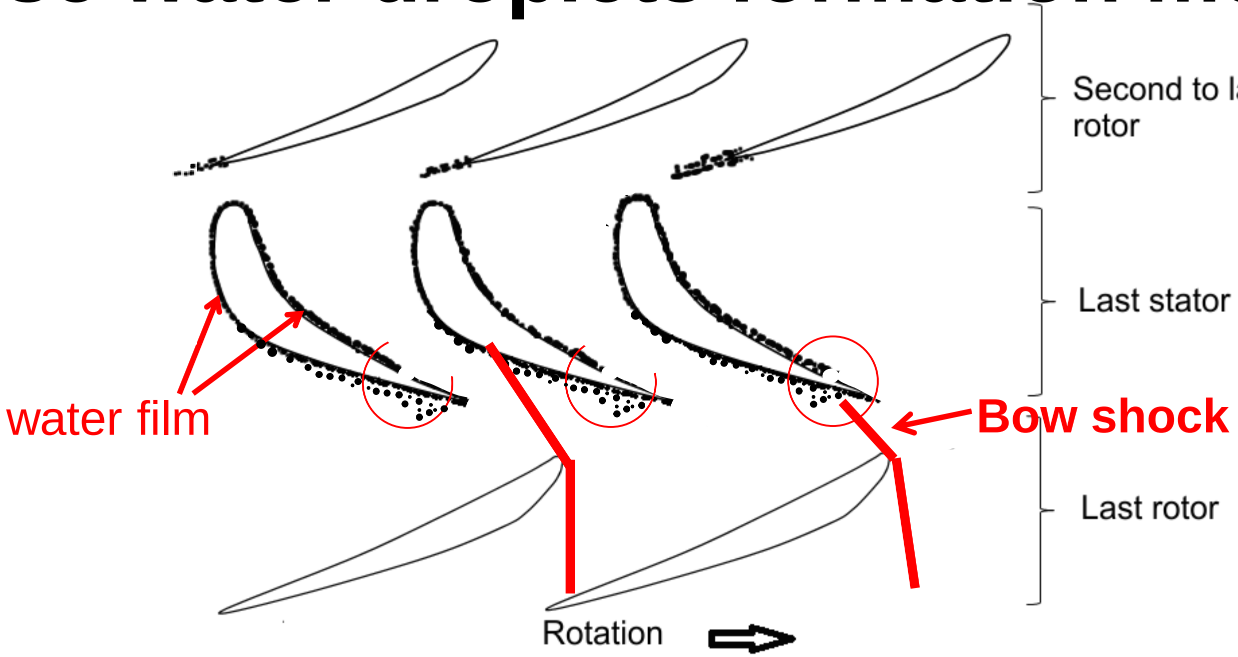

Water droplet paths and film formation in the last stage of a LP steam turbine (Moore and Sieverding)

- Coarse droplets responsible for erosion appear downstream of the trailing edge due to film breakdown or/and due to coagulation in the main stream flow
- Water film is built on both sides of the last stator
- Coarse droplets results with FRAP-OB at the stator exit showed:
  - Pressure side→ suction slit removes water content
  - Suction side→ coagulation from upstream stator wake due to turbulent mixing / free surface atomization (water film instabilities triggered by rotor potential field)

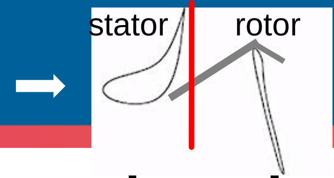

Correlation of coarse droplets with turbulent mixing

Droplet rate [mg/rev] @ 78% span

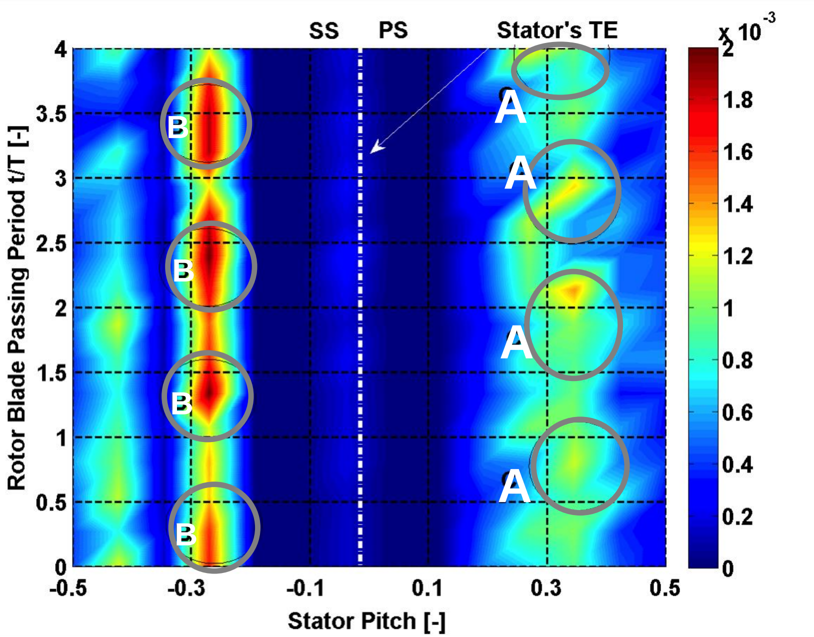

Streamwise vorticity [-] @78% span

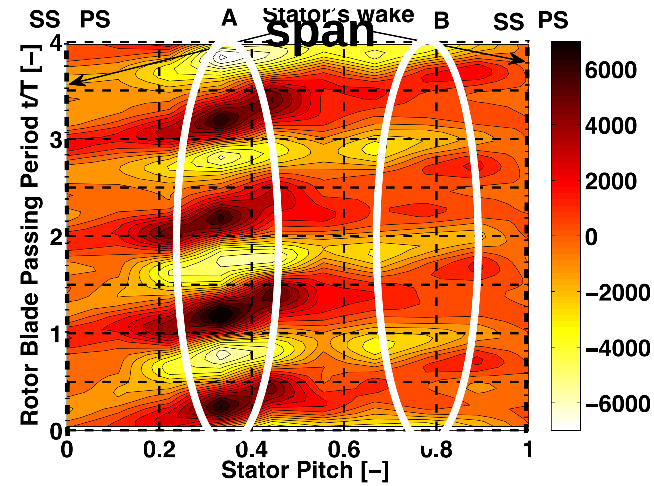

Cps [-] @78% span

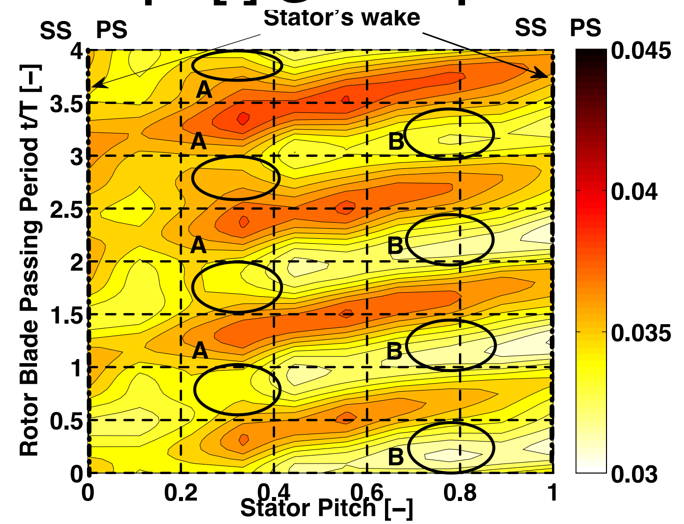

- Regions of high water content (A & B)
  - High alternating streamwise vorticity (A & B)
  - Low static pressure (A & B)
- Regions of high vorticity are associated to regions of high turbulent mixing in the flowfield

Motivation

- Motivation:
  - Knowledge of the local wetness fraction allows calculation of efficiency

$$\eta = \frac{h_{in} - h_{ex}}{h_{in} - h_{ex,is}} \text{ with } h_{ex} = h_{ex,sat}(1 - Y) + h_{ex,w} Y$$

- Objectives:
  - Develop optical extinction probe with high power density heater
  - Processing Code development
    - Extract droplet size distribution and concentration from spectral transmission data
  - Measurements in real droplet suspension environment
    - Verification measurements in characterized spray

Optical Extinction Probe (FRAP-OE)

- Probe tip diameter: Ø9.4mm (smallest ever reported)
- Measurement range: 0.2 µm to 10 µm
- Spectrometer resolution: 0.5nm
- Light source power: 240 W, λ: 400nm – 800nm
- Overall probe length: 1 m
- Max sampling frequency: 1000Hz
- High density heater installed: 38W/cm³

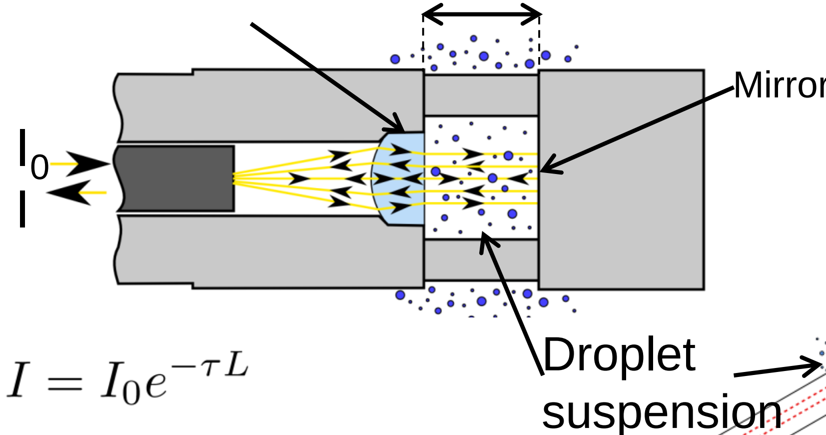

$$I = I_0 e^{-\tau L}$$

$$\frac{1}{L}\ln\left(\frac{I_0}{I}\right)\bigg|_{\lambda=\lambda_i} = \int_0^{\infty} D^2 \frac{\pi}{4} E(\lambda_i, D) N(D) dD$$

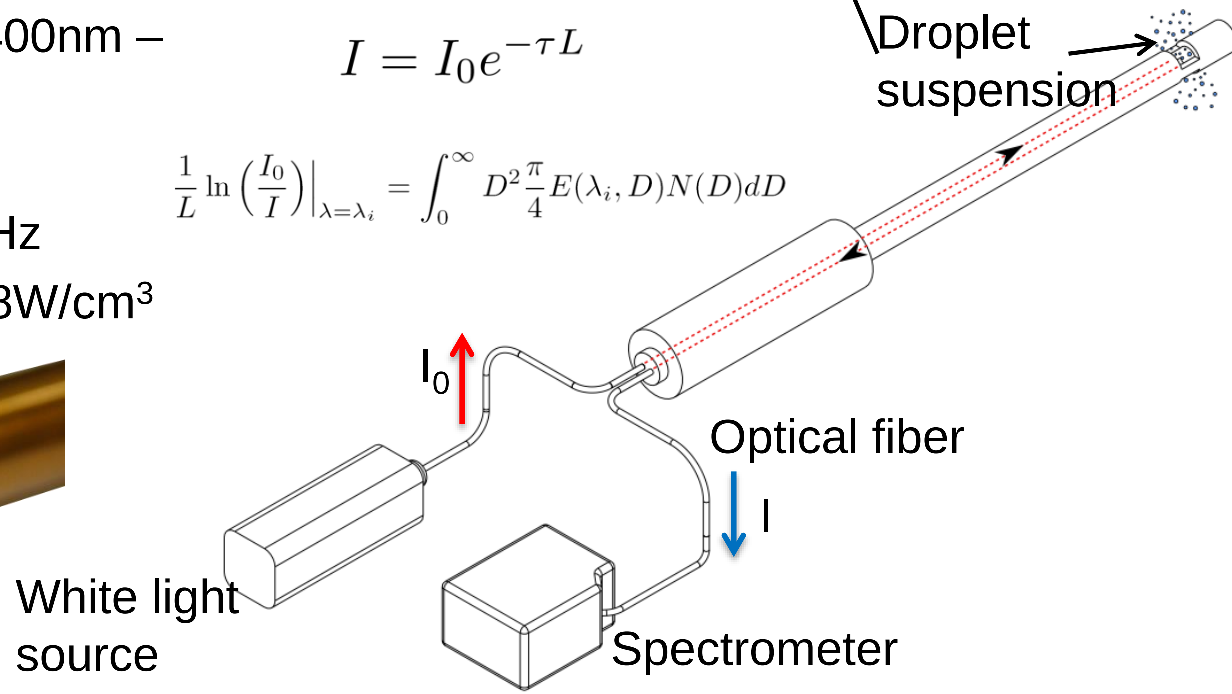

Optical Backscatter Probe (FRAP-OB)

Theoretical Background

- From Theory: The relation of transmission ln(I/I0) and droplet size distribution N(D) at a wavelength λ0 along a path L is known :

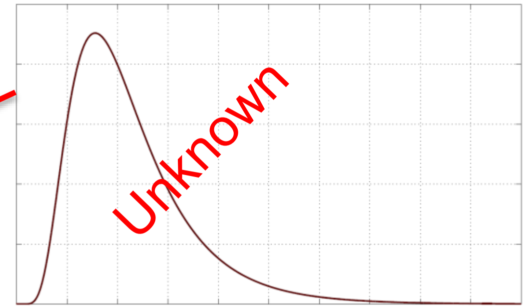

$$\frac{1}{L}\ln\left(\frac{I_0}{I}\right)\bigg|_{\lambda=\lambda_i} = \int_0^{\infty} \frac{\pi}{4} D^2 N(D) E(D,\lambda_i)dD$$

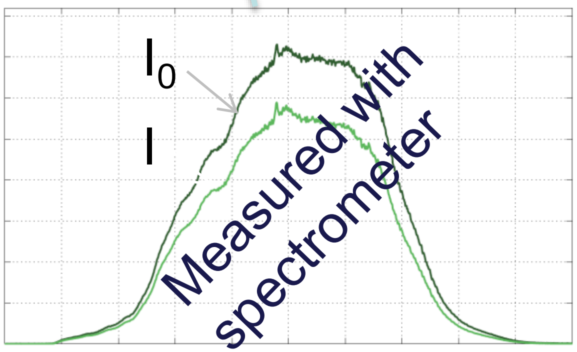

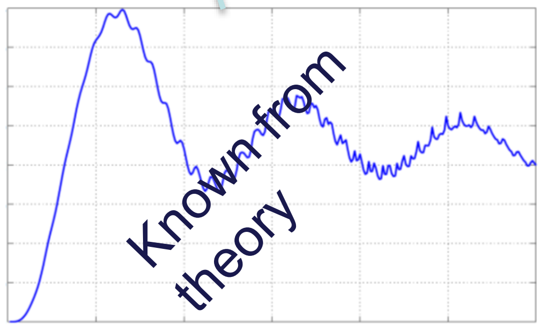

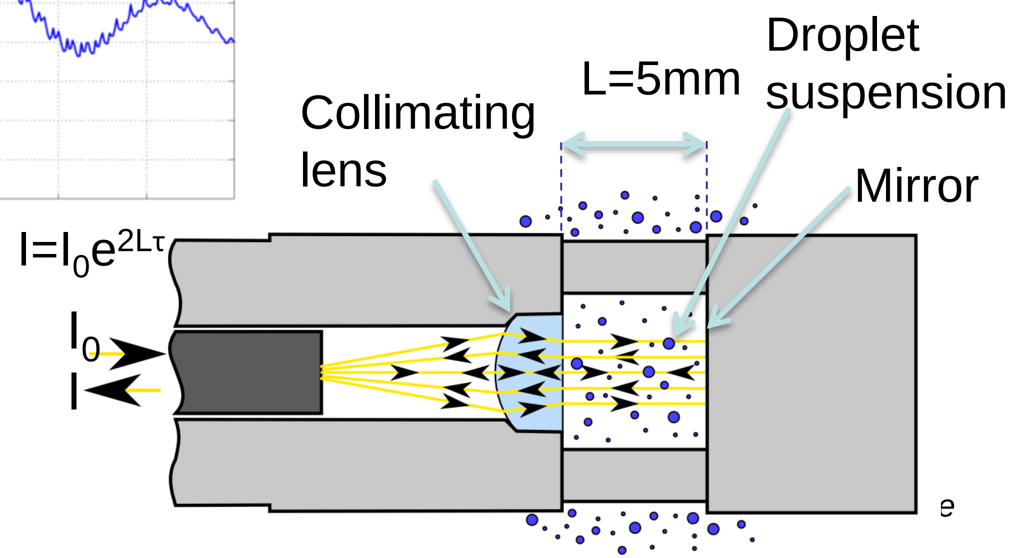

- Size distribution is extracted by solving the Fredholm integral equation numerically
- Limitation: D_{max} π/λ<30

Optical Extinction Probe (FRAP-OE)

Matrix Inversion Approach (Twomey–Non Negative Least Square algorithm)

- Transform integral into a weighted sum with gauss quadrature:

$$\frac{1}{L}\ln\left(\frac{I_0}{I}\right)\Big|_{\lambda=\lambda_i} \approx \sum_{j=1}^{N} w_j D_j^2 \frac{\pi}{4} E(\lambda_i, D_j) N(D_j)$$

- This allows to represent the equations in matrix form

$$\begin{bmatrix} \frac{1}{L}\ln\left(\frac{I_0}{I}\right)\Big|_{\lambda=\lambda_1} \\ \frac{1}{L}\ln\left(\frac{I_0}{I}\right)\Big|_{\lambda=\lambda_2} \\ \vdots \\ \frac{1}{L}\ln\left(\frac{I_0}{I}\right)\Big|_{\lambda=\lambda_k} \end{bmatrix} = \begin{bmatrix} w_1 D_1^2 \frac{\pi}{4} E(\lambda_1, D_1) & w_2 D_2^2 \frac{\pi}{4} E(\lambda_1, D_2) & \dots & w_N D_N^2 \frac{\pi}{4} E(\lambda_1, D_N) \\ w_1 D_1^2 \frac{\pi}{4} E(\lambda_2, D_1) & w_2 D_2^2 \frac{\pi}{4} E(\lambda_2, D_2) & \dots & w_N D_N^2 \frac{\pi}{4} E(\lambda_2, D_N) \\ \vdots & \vdots & \ddots & \vdots \\ w_1 D_1^2 \frac{\pi}{4} E(\lambda_k, D_1) & w_2 D_2^2 \frac{\pi}{4} E(\lambda_k, D_2) & \dots & w_N D_N^2 \frac{\pi}{4} E(\lambda_k, D_N) \end{bmatrix} \begin{bmatrix} N(D_1) \\ N(D_2) \\ \vdots \\ N(D_N) \end{bmatrix}$$

Measured g Known from theory and quadrature $\boldsymbol{A}$ Unknown f

- This matrix equation can **not** be solved directly because of extinction matrix is close to singularity causing fluctuating and unfeasible solutions
- A smoothing matrix H is introduced to the regularized non negative least square problem

$$min\left\{\|\boldsymbol{A}f - g\|^2 + \gamma f' \boldsymbol{H} f\right\}, \text{with } f_i \geq 0$$

→ Minimize residuals and roughness generates a feasible solution non negative solution

Residual norm Smoothing factor Smoothing matrix

Smoothing Parameter Optimization: L-Curve Approach

- Smoothing parameter influences solution shape
- Optimal choice is crucial
- L-Curve approach: Optimal choice of γ
- When smoothness changes less than residuals, an optimal choice is reached

$$\min\left\{\underbrace{\|\boldsymbol{A}f-g\|^2}_{\text{Residuals}}+\gamma\, \underbrace{f'\boldsymbol{H}f}_{\text{Smoothing matrix}}\right\}, \text{with } f_i \geqq 0$$

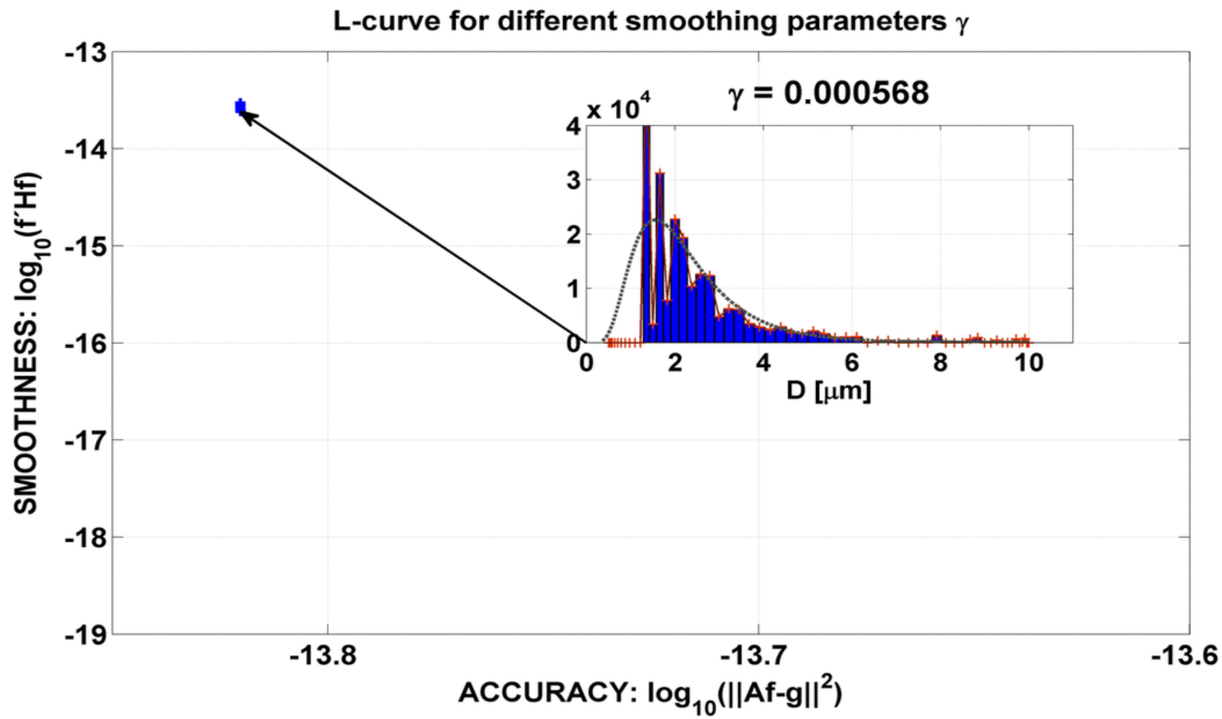

Fine Droplet Spray Characterization using Phase Doppler Anemometry (PDA) System: Results

- Five sprays were characterized at three different axial locations from the nozzle exits.
- Droplet size and velocity distributions were measured
- 2 out of 5 sprays generate droplets on the interested range of D<10µm
- Wetness fraction and concentration were calculated in a second step

PDA Measurement volume

Receiving optics

Ultrasonic atomizer

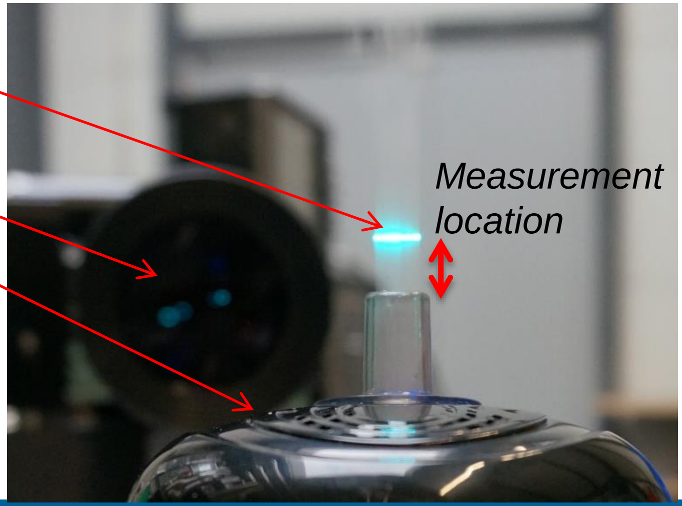

Ultrasonic atomizer: L=20mm

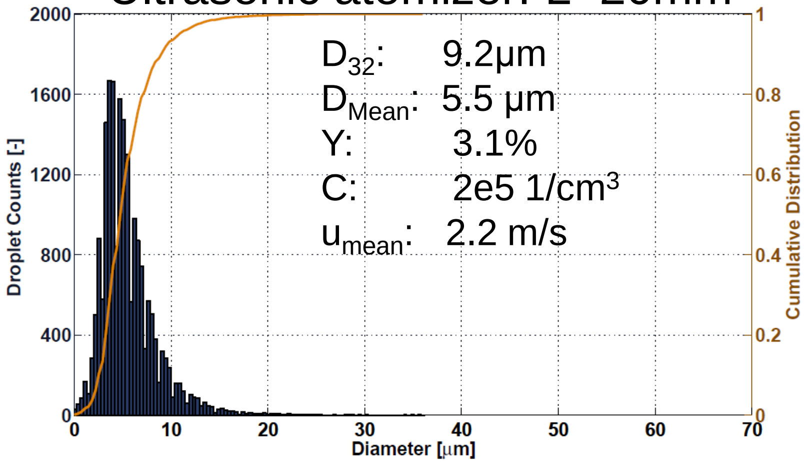

Steam generator: L=70mm

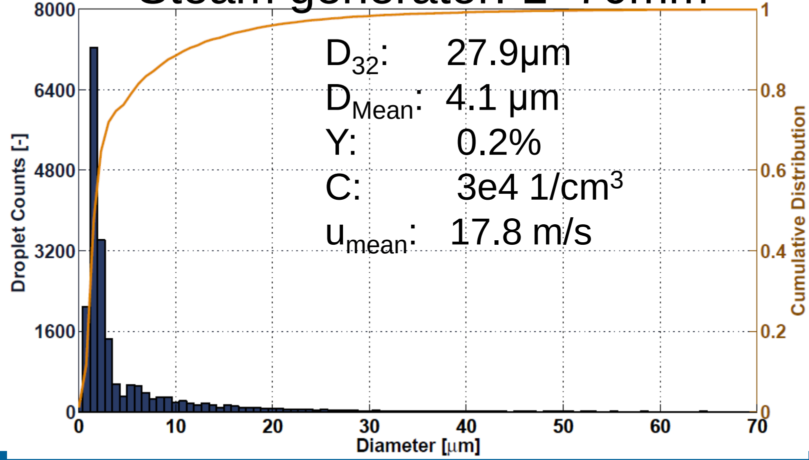

Results with Ultrasonic Atomizer: 40mm Axially Downstream

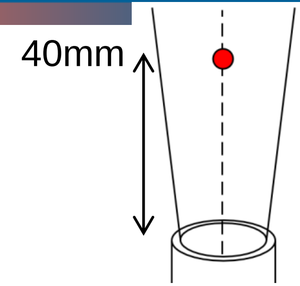

- Good agreement in the reliable PDA measurement range of D> 4µm
- Discrepancy in range of D< 4 µm
- Match in diameters: ΔD < 2.5 µm
- Wetness fraction discrepancy: 0.3%
- OEP shows a higher concentration due to the different measurement principle and limited measurement range of D<4 µm

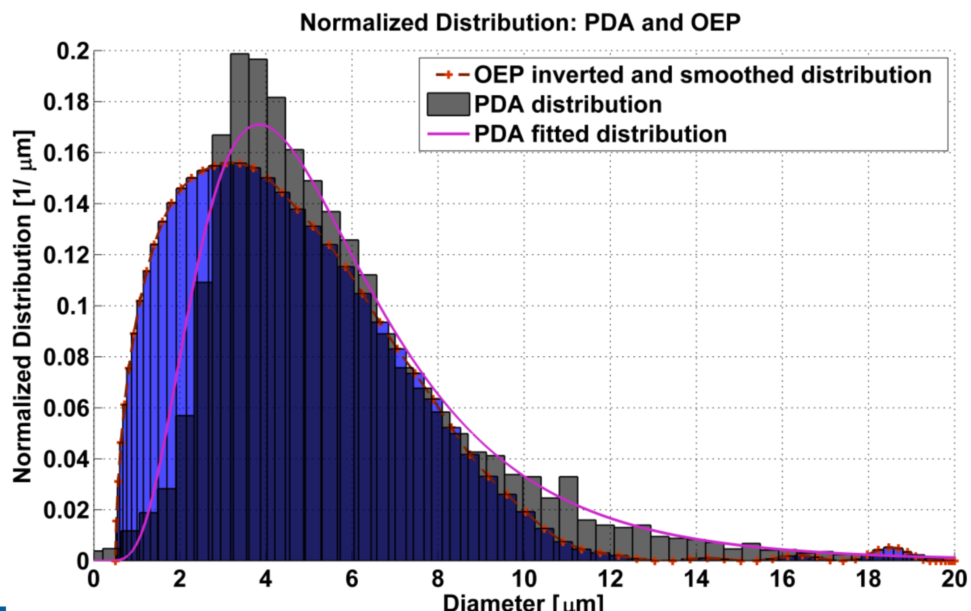

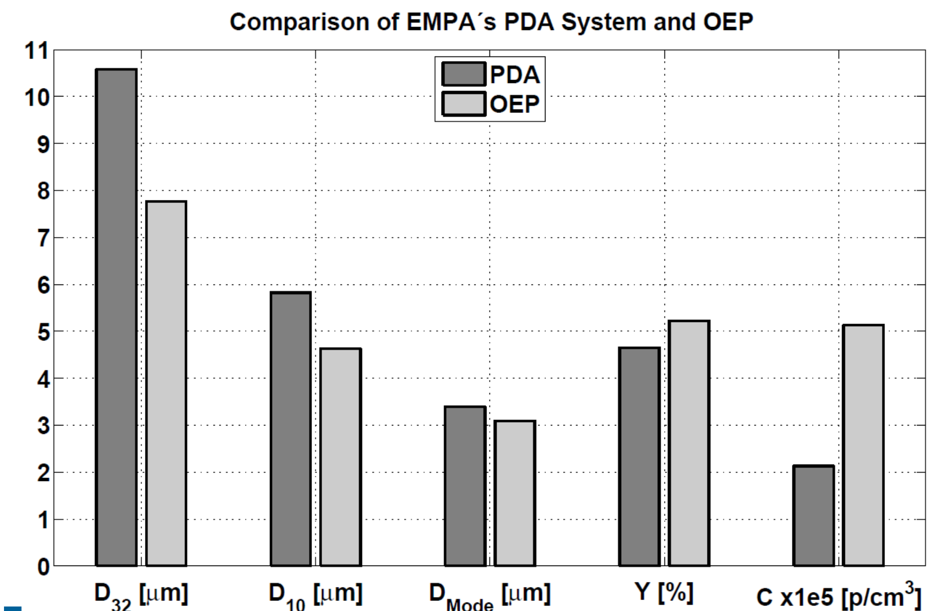

Calibration Facilities & Services
キャリブレーション施設 及び サービス

Sensor Calibration Oven

- Pressure & temperature sensors
- $0.01 \le p \le 4000$mbar
- $10 \le T \le 260^\circ$ C
- 24bit resolution ADC

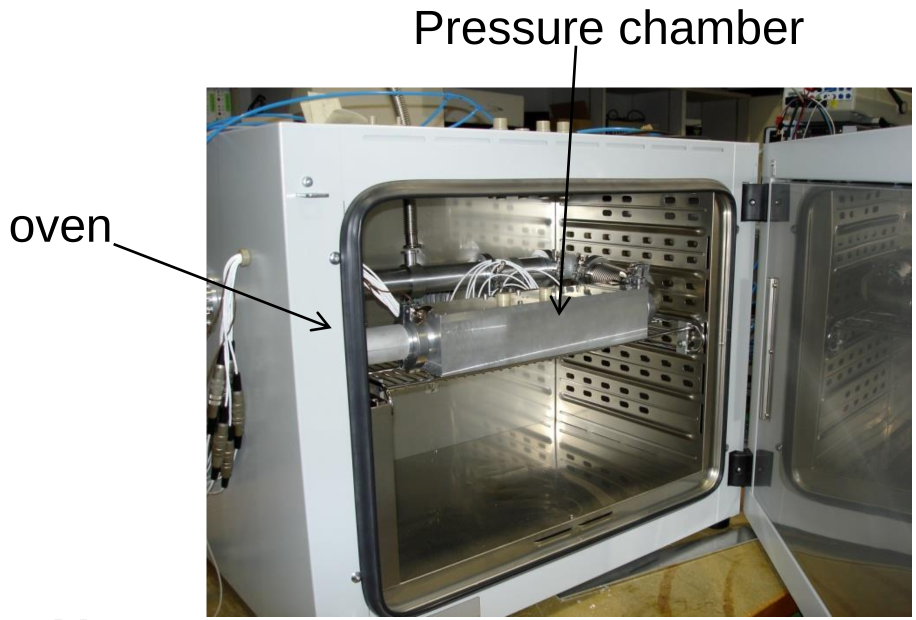

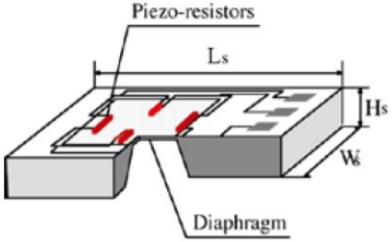

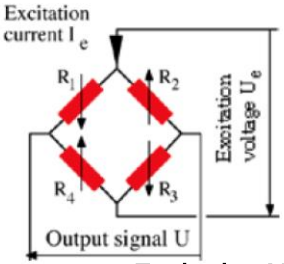

Pressure Voltage [V]

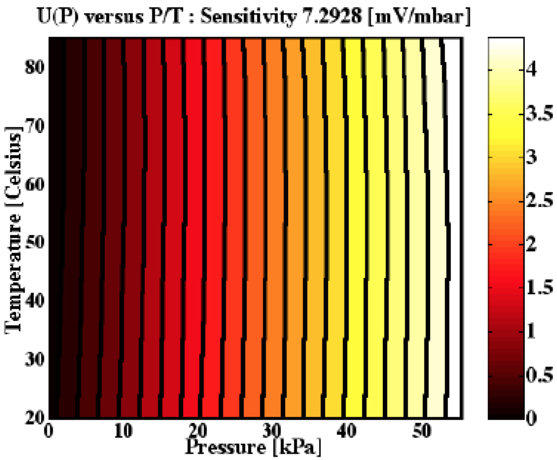

Excitation Voltage [V]

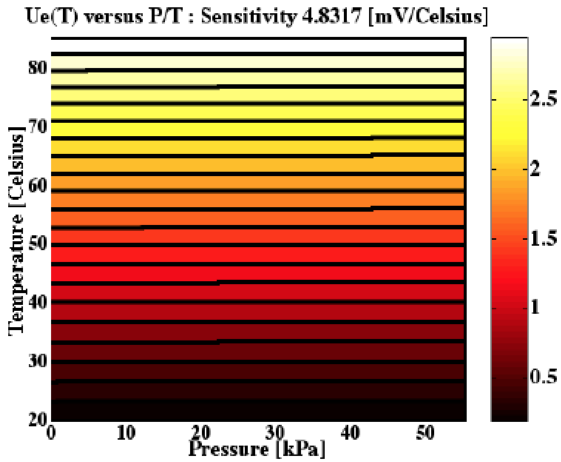

$$P(U, Ue) = \sum_{i=0}^{n} \sum_{j=0}^{m} k_{ijP} \cdot U^i \cdot Ue^j$$

$$T(U, Ue) = \sum_{i=0}^{n} \sum_{j=0}^{m} k_{ijT} \cdot U^i \cdot Ue^j$$

Virtual 4-sensor mode

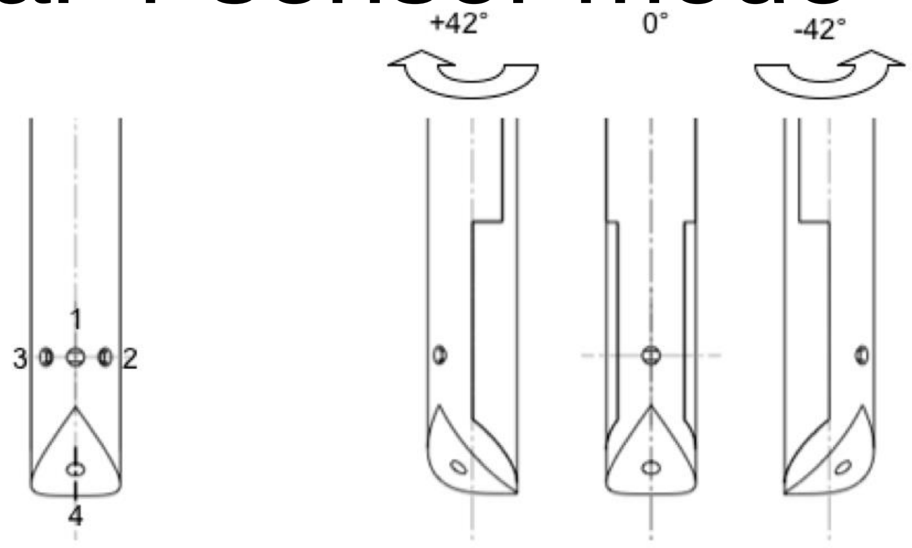

Yaw calibration coefficients K_{Phi}:

$$K_{Phi} = \frac{P_2 - P_3}{P_1 - \frac{P_2 + P_3}{2}}$$

Pitch calibration coefficients K_{Gamma}:

$$K_{Gamma} = \frac{P_1 - P_4}{P_1 - \frac{P_2 + P_3}{2}}$$

Total pressure calibration coefficient K_t:

$$K_{tot} = \frac{P_{tot} - P_1}{P_1 - \frac{P_2 + P_3}{2}}$$

Static pressure calibration coefficient K_s:

$$K_{stat} = \frac{P_{tot} - P_{stat}}{P_1 - \frac{P_2 + P_3}{2}}$$

“Freejet” Aeroalibration Facility

- Automated calibration facility
- Flow angle range: ±30° (extended ±60°)
- Mach ≤ 0.9

$$\varphi = \sum_{i=0}^{n} \sum_{j=0}^{m} k_{ij\varphi} K_{\varphi}^{i} K_{\gamma}^{j} \qquad K_t = \sum_{i=0}^{n} \sum_{j=0}^{m} k_{ijt} \varphi^{i} \gamma^{j}$$

$$\gamma = \sum_{i=0}^{n} \sum_{j=0}^{m} k_{ij\gamma} K_{\varphi}^{i} K_{\gamma}^{j} \qquad K_s = \sum_{i=0}^{n} \sum_{j=0}^{m} k_{ijs} \varphi^{i} \gamma^{j}$$

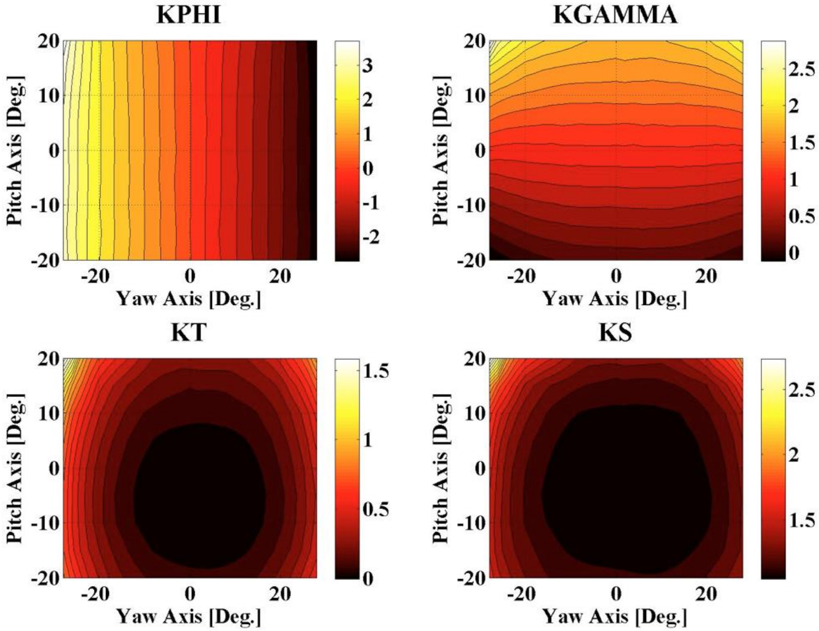

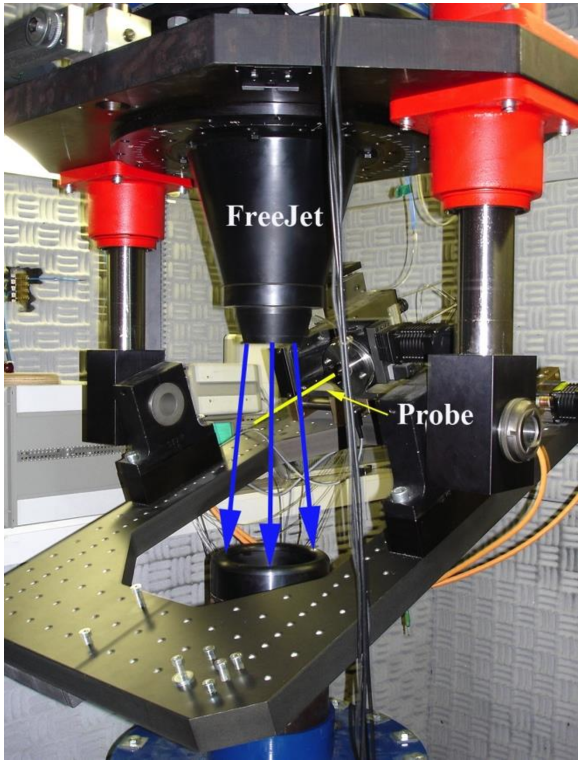

- Polynomial interpolation scheme
- Multimach number model
- incompressible &
  compressible flow regimes

"Shock Tube" Dynamic Calibration Facility

- Equipped with fast trigger and reference pressure sensor
- Transfer function characterization (Amplitude & Phase)
- Allows Numerical compensation towards measurement bandwidth extension

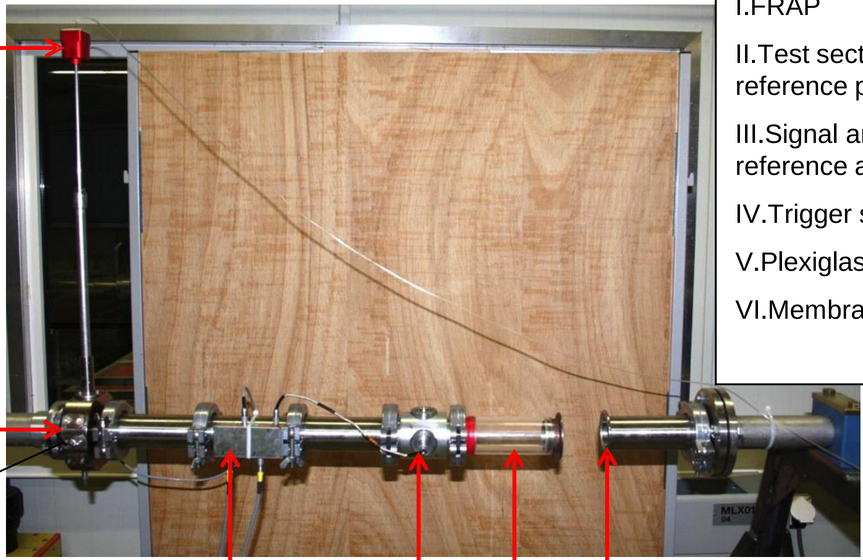

Legend:

I.FRAP

II.Test section of FRAP and reference probe

III.Signal amplifier of reference and trigger sensor

IV.Trigger sensor

V.Plexiglas tube

VI.Membrane section

New reference fast-pressure sensor

FRAP-2S Transfer Function

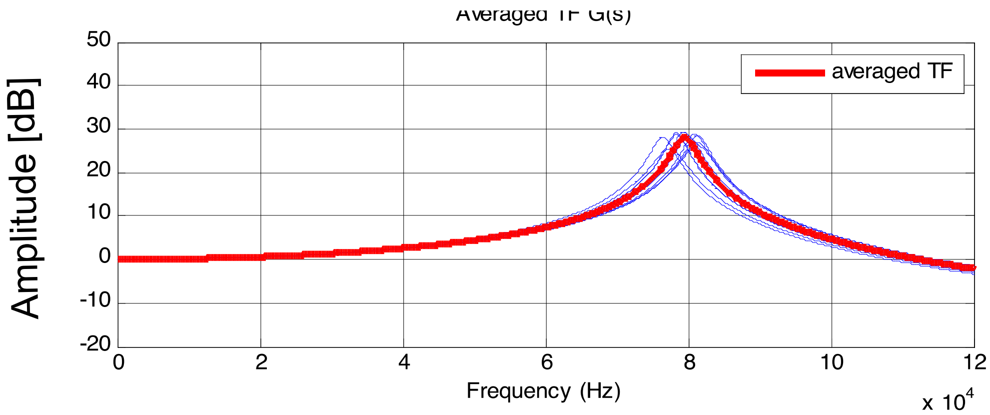

Concluding Remarks

- Develop miniature fast-response probes and sensors technology with wider measurement capabilities
- Enabling optimized turbomachinery design
  - Turbine aerodynamics
  - Aero-thermal design
  - Aero-mechanical performance
  - Accurate experimental data base
  - Effective and Targeted unsteady Modeling
- Engineering services for measurement campaigns and new blading design

Thank you for your attention!